IOSR Journal of Dental and Medical Sciences (IOSR-JDMS)
e-ISSN: 2279-0853, p-ISSN: 2279-0861.Volume 20, Issue 1 Ser.13 (January. 2021), PP 42-73
www.iosrjournals.org

Utility of Perfusion Weighted MRI and MR Spectroscopy in Intra Cerebral Glioma Grading

Dr p.Shalinidevi, am a M.D.
Trainee in the Department of Radiodiagnosis with the following particulars
Md Radio-Diagnosis
Sri Venkateswara Institute of Medical Sciences Tirupati, Andhra Pradesh.

Dr. A .Y. Lakshmi M.D.
RADIODIAGNOSIS Professor and Head, Department of Radiology, SVIMS, Tirupati

Dr. V.V.Ramesh Chandra, M.S. MCH
Professor and Head, Department of Neurosurgery, SVIMS, Tirupati

Dr. Rukmangada, M.D
Professor and Head, Department of Pathology SVIMS, Tirupati

Abstract:
Back ground: Perfusion weighted MRI and MR Spectroscopy are advanced non-invasive imaging techniques.Advanced MR imaging techniques provide physiological information which complements the conventional imaging findings in preoperative glioma grading. Histopathology is gold standard, but invasive technique. Relative cerebral blood volume (rcbv) measurements derived from perfusion MR imaging and metabolite ratios from MR spectroscopy are useful in predicting glioma grading.
AIM: *To evaluate the role of Perfusion weighted MRI and MR SPECTROSCOPY in preoperative grading of gliomas.*
Materials And Methods: *Fifty patients with primary cerebeal glioma underwent MR perfusion and MR Spectroscopy pre-operatively.The rcbv measurements were obtained from enhancing areas or FLAIR hyperintensities. Metobolite ratios (Cho/CR, Cho/NAAand NAA/Cr) were measured at Te 30 and 135ms.Tumor grade determined with the two methods was then compared with that from histopathological grading. Receiver operating characteristics analysis were performed to determine the optimum thresholds for tumor grading. Sensitivity, specificity, PPV and NPV for identifying high-grade gliomas were also calculated.*
Results: *Statistical analysis demonstrated a threshold value of1.54 for rcbv to provide sensitivity, specificity, PPV and NPV of84.8%,82.4%.90.3% and 73.6%respectively.Threshold values of 1.65 for cHo/cr and 1.42 for Cho/NAA provided the minimum c1,c2 errors, for determining the high-grade glioma.The combination of rcbv,Cho/Cr and Cho/NAA resulted in Sensitivity,specificity,PPV and NPV of 100%,76.5%,89.2% and 100% respectively.Statistically significant difference were noted in rcbv,Cho/Cr.Cho/NAA and NAA/Cr ratios between low-grade and high-grade glioma.($p<0.005$)*
Conclusion: *The rcbv measurements and metabolite ratios both in combination can increase sensitivity,specificity and NPV, when compared with PWI alone or MRS alone in detern=mining glioma grade.Threshold values can be used in a clinical setting to evaluate tumors preoperatively for histologic grade and provide a means for guiding treatment and predicting postoperative patient outcome.*

Date of Submission: 07-01-2021 Date of Acceptance: 23-01-2021

I. Introduction

INTRODUCTION:

Gliomas are the most common primary brain neoplasms. Glioblastoma multiforme (WHO IV) is the most common malignancy among Gliomas. It accounted for28% of intracranial tumors but 80% of malignant tumors. (1) Gliomas are showing histologic findings that may vary from low grade (pilocytic astrocytoma, SEGA,Diffuse infiltrating astrocytoma) to high grade (Anaplastic astrocytoma,Glioblastoma multiforme). Prognosis and management of the disease depend on grading. The prediction of high-grade gliomas remains grave, with a mediansurvival less than 5 years for anaplastic glioma and approximately 14.5–16.6 months for Glioblastoma multiforme. (2, 3)

Accurate glioma grading is essential for clinical decision making and management. The histopathology is currently the gold standard for glioma grading in clinical practice. However, it had disadvantages like inherent sampling bias, invasive procedure, and interobserver variability. Biopsy specimens may not be representing tumor tissue sometimes due to the improper resection and intra tumoral heterogeneity. It is essential to establish an accurate diagnosis without biopsy in case of the lesion is located in critical functional brain areas or requires no surgical removal and patients are in poor general condition. (4)

Conventional structural MRI techniques are noninvasive, but they are insufficient for accurate glioma grading due to the non -specific patterns and extent of contrast enhancement. (5) Up to 45% of non -enhancing gliomas are malignant, and approximately 20% of improving oligodendrogliomas are benign. (6)

Conventional MR imaging provides essential information about contrast material enhancement (break down of blood-brain barrier), edema, hemorrhage, necrosis, mass effect, and so on, which are all helpful in characterizing tumor severity (represent high -grade). (7)However, contrast material enhancement alone is not always accurate in predicting tumor grade. The mass effect and necrosis are the two most important predictors of tumor grade. The peritumoral hyper intensity on conventional T2-weighted MR images are nonspecific: it may be due to tumor infiltration, vasogenicedema, or both. So conventional M.R. imaging does not provide any reliable information.

Advanced MR imaging techniques such as perfusion M.R. imaging and proton M.R. spectroscopy have increased glioma grading utility. Both are non- invasive procedures. Relative cerebral blood volume (rCBV) maps and measurements have been shown to correlate with tumor grade and histological findings of increased tumor vascularity in Perfusion MRI. (8)

M.R. spectroscopy measures chemical composition and metabolism of the tumor. Specifically, elevation in choline (Cho) with depression of N-acetyl aspartate (NAA) is a reliable indicator of a tumor. The metabolite ratios of Cho/creatine (Cr), Cho/NAA, NAA/Cr, and Myo-inositol/Cr and the presence of lipids and lactate also useful in grading tumors and predicting tumor malignancy.(9) Metabolite ratios correlate with KI -67(proliferative marker) in histopathology. KI-67 is more in high-grade gliomas. MRS measures lipid and lactate levels inhigh-grade gliomas.

The role of necrosis is important indifferentiating from anaplastic astrocytoma (Grade3) to GBM (Grade4) and plays an essential role in the grading.

Need for the study:

The present study was taken up to evaluate PWI and MRS's accuracy in the grading gliomas, as grading plays an essential role in further management.

II. Aim And Objectives

AIM OF THE STUDY:

- To evaluate the role of Perfusion weighted MRI and MR SPECTROSCOPY in preoperative grading of gliomas.

OBJECTIVES OF THE STUDY:

- To preoperatively grade gliomas using perfusion MRI parameters.
- To preoperatively grade gliomas using M.R. spectroscopy.
- To evaluate preoperative MRI grading with histopathological grading on postoperative/biopsy specimen.
- To evaluate which parameter in PWI and MRS is more useful in preoperative grading.

III. Review of Literature

REVIEW OF LITERATURE:

Classification and grading of the brain tumors

The most widely accepted classification of brain neoplasms is sponsored by the World Health Organization (WHO). Since 1986, a working group of world-famous neuropathologists has convened approximately every seven years for an editorial and consensus update conference on brain tumor classification and grading. The results are then published by the International Agency for Research on Cancer (IARC) as the WHO Classification of Tumors of the Central Nervous System. The fourth edition was published in 2007 and added eight new tumor entities plus four new variants to the existing classification schema. It was based on the concept that tumors could be classified according to their phenotypic similarities with different putative cells of origin. These were mostly microscopic features and immunohistochemical (IHC) expression of lineage-associated proteins. They were then graded on a scale of I-IV according to their observed level of Differentiation. (10)

After 8 years, an update of the central nervous system of tumors was published in 2016 after 2007. The 2016 WHO classification incorporate both genotypic and phenotypic (i.e., histological) parameters. (10) There are two significant ways to identify the genetic signatures of brain tumors. By (1), direct interrogation of the mutated DNA itself,it is relatively expensive and unavailable at many medical centers. (2) Immunohistochemistry, which assesses the effects of the mutated genes on proteins. Grading is used to predict the biologic behavior of tumors and together with molecular features, remains an essential guide to therapeutic decisions.

CNS tumors peaks among young children (those aged more youthful than fiveyears) and then again in the fifth to seventh decades of life. CNS tumors are now the second leading cause of cancer-related mortality in men aged 20-39 years and the fifth leading cause in women. Meningiomas are the most common histological subtype of primary CNS neoplasm, followed by gliomas and pituitary adenomas. (11)

GLIOMAS:

Glial neoplasms constitute one of the most heterogeneous brain tumors and are the most common overall malignant brain tumor. Tumors of putative glial cell origin were called initially "gliomas" (because of their supposed derivation from glue-like glial cells). The neuropil contains several subtypes of glial cells: astrocytes, oligodendrocytes, ependymal cells, and modified ependymal cells that form the choroid plexus. In the past, each subtype was thought to give rise to a specific type of "glioma."

Now, the brain parenchyma's primary neoplasms are thought to arise from pluripotential neural stem cells (NSCs).These NSCs persist in two areas of the postnatal brain: the subventricular zone—the region located under the brain ventricles' ependyma—and the dentate gyrus of the hippocampus. Brain NSCs have a high rate of proliferation and are thus prone to genetic errors. When these brainstem cells mutate, they become tumor progenitor cells (tumor stem cells) that can generate phenotypically diverse neoplasms. (12, 13)

ASTROCYTOMAS:

Astrocytoma’s probably develop from distinct populations of precursor "glioma-initiating" cells that possess stem cell properties.Astrocytoma’s can be relatively localized (and generally behave more benignly) or diffusely infiltrating with an inherent tendency to malignant degeneration. Diffuse astrocytoma’s are now divided into IDH-mutant and IDH-wild-type tumors.IDH mutants are showing a good prognosis.(14) Only two are relatively localized histological subtypes of astrocytoma’s—pilocytic and subependymal giant cell astrocytoma’s—are designated as WHO grade I neoplasms. All diffusely infiltrating astrocytoma’s are at least WHO grade II neoplasms, and the vast majority is grading III-IV.

Tumors with cytological atypia alone (i.e., diffuse astrocytoma’s) are considered WHO grade II. If anaplasia and mitotic activity are also present, they are considered WHO grade III (i.e., anaplastic astrocytoma).Tumors that additionally demonstrate microvascular proliferation (defined either as endothelium (14) multilayering—not simple hypervascularity—or "glomeruloid" vasculature) or necrosis are WHO grade IV neoplasm’s (i.e., glioblastoma). Distinguishing a grade II from a grade III astrocytoma based onhistological features alone can be difficult. Neuropathologists add a measure of cellular proliferation called the Ki-67 proliferation index as a surrogate estimate for subsequent biologic behavior of the tumor. (15,16)

Figure 1: origin of various grades of glial tumors from Glial progenitor cells

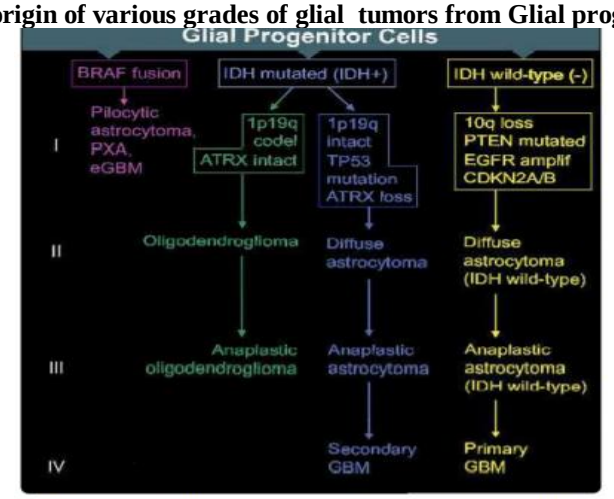

(17-1) Glioma cell lines are shown with "driver" mutation IDH+. Subsequent mutations lead either to astrocytomas (blue) or oligodendrogliomas (green). IDH-wild-type astrocytoma grades II/III lead to primary glioblastoma (GBM).

Imaging features of astrocytoma's :

DIFFUSE ASTROCYTOMAS WHO grade 11:

Diffuse astrocytoma's are hypodense on NECT and not showing enhancement on CECT.On MRI, they appear as hypointense on T1, hyperintense on T2/FLAIR and not showing enhancement on the post-contrast study. LowrCBV on PWI. Foci of increased rCBVare suspicious for malignant degeneration. (16)

ANAPLASTIC ASTROCYTOMA WHO grade 3:

Imaging features like diffuseastrocytomas but may show enhancing focus. Any areas of increased rCBV likely represent malignant degeneration.

GBM WHO grade IV:

IDH-Wild-Type GBM: Also called "primary" GBM. It Arises as de novo, showing IDH1 negative, PTEN mutation and EGFR amplified. It constitutes > 95% of all GBMs. The peak age of occurrence is 55-85 years with Survival< 1 year. It occurs anywhere in hemispheres showing thick irregular enhancing tumor "rind" around the central necrotic core, and hemorrhage is common. (16)

IDH-Mutant GBM: Also called "secondary," GBM arises from malignant degeneration of lower-grade tumors. Mutant type is showing IDH1 mutation and TP53 mutation, ATRX lost. It constitutes 5% of GBMs. The peak age of occurrence is 45 years with Survival rate is 2-3 years. Pathology is Similar to IDH-wild-type but shows less palisading necrosis. They show predilection for frontal lobe with less prominent necrosis. On imaging,it showing significant non-enhancing areas.(16)

Nonastrocytic Glial Neoplasm's

Oligodendroglial Tumors:

Oligodendroglial tumors are IDHmutant and have a specific mutation, 1p19q co-deletion. Two grades are recognized: a well-differentiated WHO grade II neoplasm (oligodendroglioma) and a WHO grade III neoplasm (anaplastic oligodendrogliomas). 85-90% occurrence in cerebral hemispheres (most common = frontal lobes) arises at grey-white matter junction and diffusely infiltrate cortex. Microscopic features are "Fried egg" cells with "chicken-wire" vascularity noted. On imaging shows calcifications 70% and hemorrhage, edema is uncommon, and 50%may show enhancement. (17)

Ependymal Tumors:

Ependymal tumors vary from WHO grade I to III. Sub ependymoma grade I tumor, a benign-behaving neoplasm of middle-aged and older adults that occurs in the frontal horn. Myxopapillary ependymoma grade 1 tumor, a tumor of young and middle-aged adults almost exclusively found at the CONUS, cauda equina, and filum terminale of the spinal cord. Ependymoma, generally a slow-growing tumor of children and young adults, is a WHO grade II neoplasm that may arise anywhere along with the ventricular system and in the central canal of the spinal cord. Anaplastic ependymomas are biologically more aggressive, have a poorer prognosis, and are designated WHO grade III neoplasms. Infratentorial ependymomas, typically arising within the fourth ventricle, occur predominantly in children. Supratentorial ependymomas are more common in the cerebral hemispheres than the lateral ventricle and are usually tumors of young children.A newly described tumor of ependymoma is RELA fusion-positive ependymoma. (18)

Neovascularization is a typical tumor hallmark for gliomas. Neovascularization is responsible for multiple biological behaviors such a tumor progression, invasiveness, and therapy resistance. (19) In low-grade glioma (LGG), tumor vessels are mainly composed of normal endothelial cells (E.C.s), with cell-to-cell tight junction and relatively intact blood-brain barrier (BBB).(20)However, the vascular ultrastructure of high-grade glioma (HGG) is characterized by large caliber and aberrant vascular walls, composed of abundant immature E.C.s with loose conjunctions, fenestrated structure, and discontinuous membrane. (21)The marginal tumor area is rich in proliferative and invasive cells, with increased micro vessel density (MVD) and active neovascularization. The Tumor core comprises compressed and tortuous vascular networks with reduced vascular perfusion, resulting in hypoxia, cell metabolic scarcity, and necrosis.(22, 23)

Conventional MR imaging:

Conventional MR imaging provides important information about contrast material enhancement (the breakdown of the blood-brain barrier), edema, hemorrhage, necrosis, mass effect, and so on, which are all helpful in characterizing tumor aggressiveness (represent high grade).(7)Often a high-grade glioma may be mistaken for a low-grade glioma when it demonstrates minimal edema, no contrast material enhancement, no necrosis, and no mass effect. Low-grade gliomas can sometimes mistake as high-grade gliomas, due to peritumoraledema, contrast material enhancement, central necrosis, and mass effect. However, contrast material enhancement alone is not always accurate in predicting tumor grade. That mass effect and necrosis were the two

most important predictors of tumor grade. The peritumoral hyper intensity on conventional T2-weighted MR images is nonspecific; it may be due to tumor infiltration, vasogenic edema, or both. So conventional M.R. imaging does not provide any reliable information to grade CNS tumors.
Magnetic resonance perfusion and M.R. Spectroscopy are advanced non-invasive imaging methods often used in the diagnosis of glioma grading. Several studies support the utility of these methods, alone or in combination with others, for differentiating low grade and high-grade gliomas.

PERFUSION WEIGHTED MRI:

Cerebral perfusion is defined as the steady-state delivery of nutrients and oxygen via blood to brain tissue parenchyma per unit volume and is typically measured in milliliters per 100 g of tissue per minute. In perfusion M.R. imaging, however, the term perfusion comprises several tissue hemodynamic parameters (cerebral blood volume – CBV, cerebral blood flow – CBF, and mean transit time - MTT) that can be derived from the acquired data. In the evaluation of intracranial mass lesions, however, CBV appears to be the most useful parameter.

Vascular morphology and the degree of angiogenesis are important elements in evaluating different tumor types and determining the biologic aggressiveness of intracranial neoplasms. Tumor angiogenesis(24), can be indirectly assessed using perfusion M.R. imaging derived in vivo maps of cerebral blood volume that depict the overall tumor vascularity.M.R. imaging measurements of relative cerebral blood volume have been shown to correlate with both conventional angiographic assessments of tumor vascular density and histological measures of tumor neovascularization to grade the gliomas.(24,25) Increased tumor vascularity, however, is not synonymous with malignancy. Several intracranial neoplasms, especially those extra-axials such as meningiomas or choroid plexus papilloma's, can be vascular but benign in biologic behavior.

In patients receiving anti-angiogenesis cancer therapies that directly attack tumor vessels, perfusion M.R. imaging is a noninvasive method to assess changes in the relative cerebral blood volume of the tumor during treatment and thus can be used to monitor the efficacy of therapy. Findings of perfusion M.R. imaging have been shown to correlate better with clinical responses of patients undergoing anti-angiogenisis treatment. (26–30)

Non- neoplastic lesions of the brain like cerebral infections, tumefactive demyelinating lesions, and less commonly, infarcts—may be confused with and misdiagnosed as brain tumors. The conventional M.R. imaging appearance of these lesions can be nonspecific and pose a severe challenge in differentiation from brain tumors. Even with a contrast agent, the distinction can be difficult because any process that disrupts the integrity of the blood-brain barrier can enhance enhancement. Potentially, perfusion M.R. imaging offers a different mechanism of differentiation by assessment of variations in vascularity of these lesions.

Principles of Perfusion weighted imaging:

Perfusion imaging with dynamic susceptibility contrast (DSC)-MRI is based on tracer kinetic modelling principles to assess the cerebral microvasculature. (31)In DSC perfusion imaging, a contrast agent is injected into the blood and monitored as it passes through the microvasculature. The vasculature is a critical feature in the histopathology diagnosis of gliomas and permits imaging associations with grade through perfusion-weighted imaging. Blood vessels are present in higher numbers within tumors than in normal brain tissue, and they tend to have a larger volume. In general, higher-grade tumors also tend to have a higher blood volume. In higher-grade tumors, the degradation and remodeling of extracellular matrix macromolecules result in loss of blood-brain barrier integrity(32, 20), which is seen as contrast leakage or enhancement. By kinetic analysis of these data, one may compute cerebral blood flow and volume and mean transit time. These measures can capture the degree of tumor angiogenesis, an essential biologic marker of tumor grade, histology, and prognosis, particularly in gliomas. Perfusion imaging is based on rapid imaging (echo-planar imaging) of the first pass of the contrast agent. It can be performed using either a gradient-echo or a spin-echo pulse sequence. In DSC imaging, the intensity decreases in more significant contrast concentration areas due to changes in local susceptibility. This differs from dynamic contrast-enhanced (DCE) MRI, in which a T1-weighted sequence detects an increase in intensity proportional to contrast concentration.

Quantitative assessment:

MRI perfusion imaging can estimate the volume of blood that passes through the capillary bed per unit of time. The quantification can be performed in a relative or absolute manner. Although absolute quantification is preferable, it is challenging to perform in clinical practice due to many potential imaging and data processing artifacts. Thus, DSC typically produces visually reviewed images, and any measurements are expressed as a ratio to normal-appearing white matter. Relative cerebral blood volume (rCBV) measurements have been shown to correlate with tumor grade and histological findings of increased tumor vascularity. (33)They have also been shown to be useful in differentiating between progression and pseudo progression. (34, 35)However, selecting

the reference region of interest (ROI) remains an open issue in clinical practice and longitudinal studies. (36)After the data are acquired, the baseline is defined; this often includes removing the first three-time points due to saturation effects. The start and endpoints of the bolus are calculated. Subsequently, the baseline signal intensity is calculated, and the signal-time curves are converted to concentration-time curves. This is done for each voxel in the imaging volume. The rCBV image is the most important of the perfusion images for analyzing brain tumors and is computed by integrating the area under the time-concentration curve. (37)Some additional image types that can be added include percent signal recovery, a measure of tumor leakiness; time to peak; bolus start and end time; and mean transit time. The latter two measures are frequently used in stroke imaging but are of limited value in tumors.

Qualitative assessment:

Several commercial software packages are available for calculating parametric maps like CBV from DSC-MRI. For routine clinical practice, visually inspecting the color maps can help to detect normal versus abnormal regions. This assessment can be very useful in the clinical setting, but it depends on the windowing technique parameters used to present the data.

BBB disruption and leakage correction:

One of the main challenges of DSC-MRI data analysis is contrast-agent extravasations due to BBB disruption. Instead of returning to baseline, the signal returns to a point higher than the initial baseline due to T1 effects, resulting in underestimating the integration area. However, depending on the pulse sequence used, T2 or T2* leakage effects can predominate, resulting in an overestimation of the rCBV value. (38)The sequence type and parameters can affect how the concentration-time curves are distorted. A one-dimensional leakage simulation study performed by Quarles et al(38),demonstrated that when T1 effects were removed, such as using a dual-/multi-echo sequence, the measured transverse relaxation-rate-time course overestimated the true transverse relaxation–rate-time course. Therefore, the CBV would be overestimated.(39) When T1 effects dominated (e.g., when the high flip angle and short repetition time were used),the measured transverse relaxation-rate-time course underestimated the true transverse relaxation-rate-time system; thus, the CBV would be underestimated. (40,41) One technique is to minimize the contrast leakage effect by administering a contrast agent before acquiring the DSC images (referred to as preloading'). However, animal studies suggest preloading is not very useful. (42,43,44)The more popular and effective method is to apply mathematical models of the leakage during DSC data analysis. (45-47)

MR SPECTROSCOPY:

Magnetic resonance spectroscopy (MRS) is a non-invasive technique to determine the molecular metabolites in any given living tissue. The metabolites are measured due to their slightly different magnetic frequencies of chemical shifts.(48) The MR spectroscopy can be considered as a method of molecular imaging. In many pathologic processes, metabolic changes precede anatomic changes during disease progression and treatment; MRS offers a way for early detection of new disease and can influence the therapeutic success or failure.(49)

The nuclei with an odd number of protons and neutrons, such as hydrogen -1 (1 proton), phosphorus -31 (15 protons and 16 neutrons), carbon -13 (6 protons and seven neutrons), fluorine -19 (9 protons and ten neutrons), have a magnetic moment and interact with the external magnetic field and are commonly used in M.R. spectroscopic studies.(50) Unfortunately, MRS can detect metabolites or chemicals in concentration more than 0.1 mM and hence is limited in terms of metabolites it can monitor. This is one of the major reasons that hindered the growth of MRS in the clinical setting despite its many promises.

PRINCIPLE: In simple MRI sequence block contains slice excitation by R.F. pulse followed by application of slice encoding, phase encoding, and frequency encoding gradients in mutually orthogonal planes. Whereas, in a classical spectroscopic imaging sequence, the MRSsignal is acquired without a frequency- encoding gradient. Consequently, in contrast to MRI, the acquired MRS signal contains different frequencies that correspond to the chemical shift and not to the signal's spatial origin. The amplitude of various metabolites' chemical shifts depends on the magnetic gyro ratio of the nuclei and intensity of the external magnetic field. So, at a given external magnetic field, every chemically distinct nucleus resonates at a slightly different frequency known as the chemical shift, which gives rise to separate peaks in the M.R. spectrum. By the same principle, in a given standard chemical environment increasing the external magnetic field strength transforms into the better separation of signal frequencies of various metabolites in the M.R. spectrum. J coupling or spin-spin coupling is due to interactions with a neighboring nuclear spin and provides additional information. (51)

MRS Spectrum: MRS provides in vivo biochemical information represented as a spectrum with the peaks in the spectra obtained correspond with various metabolites. The horizontal axis (abscissa) represents resonance frequency as parts per million to the total resonance frequency. The vertical axis plots the relative signal amplitude or concentrations for various metabolites.

The MR spectra are analyzed in the following format. (52)
1. Center of the resonance frequency in ppm
2. Peak height
3. Line width at half-height
4. Peak area and shape
5. Composition of the peaks, e.g., single, doublet, triplets.

The sharpness of the peak and line width is affected by (a) homogeneity of the external magnetic field, (b) magnetic field in homogeneity due to susceptibility gradient, and (c) T2 time of the sample (long causes narrowing of the line).

Figure 2:MR spectrum analysis

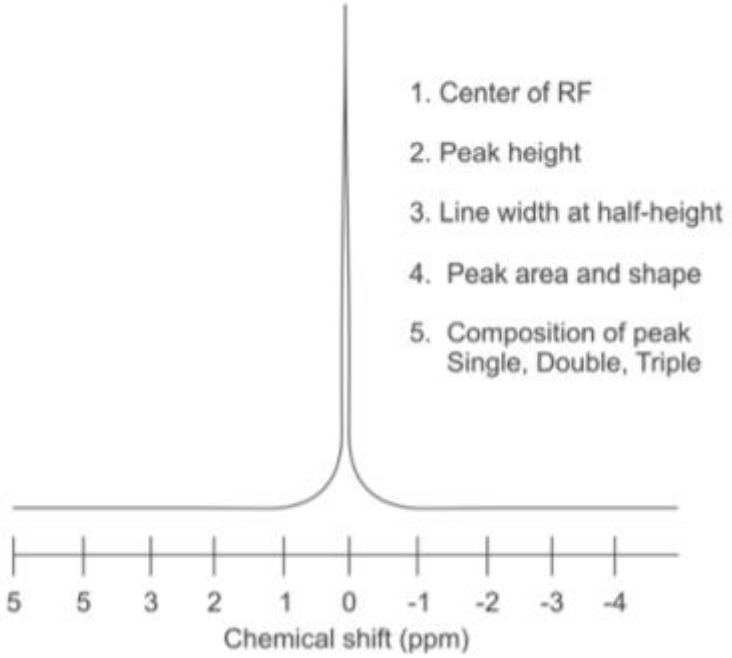

The standard conventions to display M.R. spectra include (52):
a. Up-field is to the right represents lower frequencies and are shielded
b. Down-field is to the left represents higher frequencies and are shielded.
c. Chemical shifts (in ppm) are complimentary, going to the left, and is negative towards the right.

Resonance-frequency(R.F) of a particular compound does zero setting, e.g., phosphocreatine for 31P-MRS and tetramethyl silane (TMS) for 1 H and 13C M.R.s (at 4.8 ppm). Since TMS is not seen in vivo, a known chemical like NAA at 2.0 ppm is used as chemical shift reference. The ppm scale describes the shifts in hertz from a reference peak divided by the frequency of excitation.(52)

The Proton is abundantly present in the body and hence most suited for MRS. at 1.5T, metabolites visualized utilizing intermediate to long T.E. (144- 288ms) include N-acetyl aspartate (NAA), choline (Cho), creatine (Cr), possibly alanine (Ala), and lactate. Short echo-time acquisitions (T.E. < 40 ms) include the above metabolites as well as myoinositol (Myo), glutamate and glutamine (Glx), glucose (GC), and some macromolecular proteins and lipids (52).

Figure 3: Normal proton 1 H-MRS in the brain (T.E. = 30 ms, 135ms)

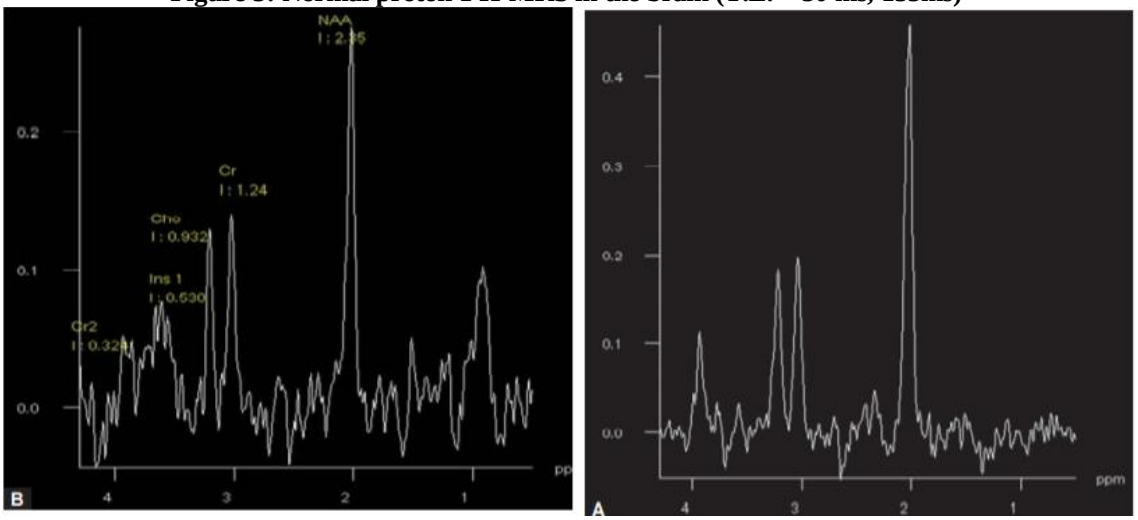

The major compounds on 1 H-MRS are. (53-55)

- N-acetyl aspartate (NAA) peak is the major up field peak on 1 H-MRS. This compound is present only in CNS, primarily in mature neurons and neuronal processes such as axons, and is a sensitive marker for neuronal viability and density.NAA resonate close to 2.0 ppm.
- The chorine (Cho) peak at 3.22 ppm is predominantly due to glycerophosphocholine (GPC) and glycerophosphoethanolamine (GPE) that form the phospholipid layer of the cell membrane. Choline increases in actively demyelinating lesions because membrane phospholipids are released during active myelin breakdown. Many brain tumors are associated with high signals from choline, presumably associated with their increased cellular density and compression of surrounding brain tissue.
- The creatine (Cr) peak at 3.02 ppm is due to the sum of creatine and phosphocreatine, and it does not indicate the energy state of the cell. Total Cr concentration is relatively constant throughout the brain and tends to be relatively resistant to change. Therefore, Cr often is used as an internal standard to which other metabolites' resonance intensities are normalized.
- Lactate peak may be seen as a doublet at 1.33 ppm and occurs due to anaerobic glycolysis. Lactate accumulates when oxidative metabolism is unable to meet energy requirements leading to accelerated anaerobic glycolysis. Certain brain tumors such as gliomas have increased lactate concentrations because they have elevated relative rates of glycolysis independent of the adequacy of oxidative metabolic pathways. Lactate tends to accumulate in the extracellular environment of necrotic tissue and fluid-filled fluid-filled cysts, and areas of ischemic infarction.
- A variety of other metabolites, including myoinositol, glutamate/ glutamine, and glucose, may also be observed. Broad peaks at 0.9-1.3 ppm of lipid may obscure some of the metabolites, contaminate the spectra, and need to be separated from lactate peak.

LOCALIZATION TECHNIQUES: There are two types of localization techniques (a) by using the main magnetic field gradient (B0 field) or (b) by using the R.F. field gradient (B1 field).

Depth-resolved surface spectroscopy (DRESS): Depth-resolved surface spectroscopy (DRESS) is the simplest gradient localization method. A single plane – selective radiofrequency (R.F.) pulse is applied to tissue volume and data acquisition. This method is crude and suffers from a lack of information at the center of R.F. pulse producing baseline artifacts. The sequence can also be used in a slice – interleaved multislice mode (SLIT-DRESS). The water suppression is achieved by using a long, low amplitude Gaussian pulse.

The pulse sequences used in single voxel spectroscopy are: (56-58)

a. **STEAM:** The stimulated – echo acquisition mode (STEAM) of localization for 1 H-MRS consists of three 90º selective pulses, each applied in the presence of an orthogonal gradient to excite a slice. This sequence is robust and straightforward, but there is approximately 50 percent signal loss.

b. **PRESS:** The point-resolved spectroscopy (PRESS) localization consists of a 90-180-180º pulse sequence, each applied in the presence of an orthogonal gradient. Unlike STEAM, it is a full signal. The PRESS sequence disadvantage is that it cannot be performed in short T.E. values (less than 40 ms) as done in the STEAM sequence. Water suppression is done by using a gaussian pulse preceding the localization pulses. This sequence variant is MESA by using binomial (1331) pulse to achieve water suppression followed by a train of three 180- 180-180º pulses.

c. **ISIS:** The image selected in vivo spectroscopy (ISIS) uses three inversion pulses and a fourth non-selective pulse to observe the signal. It requires a minimum of eight phase cycles to localize the signal. There is minimum loss from T2 relaxation and is especially useful for observing nuclei with short T2 values, such as 31P.

Chemical shift imaging (CSI)/ Multi voxel MRS(MRSI): Using phase encoding strategies, it is possible to simultaneously encode information from multiple voxels. Phase encoding can be applied in one, two, or three dimensions. Data are translated to extract chemical shift information from multiple positions using up to 4D Fourier transformations. MRSI has the advantage of obtaining multiple spectra in one data acquisition. The technique requires a homogeneous magnetic field over a larger volume than SV MRS.4 The vast quantity of data generated with CSI make management, analysis, and interpretation of CSI spectra a daunting challenge in the clinical setting.

Figure 4:Localization techniques in MR Spectroscopy

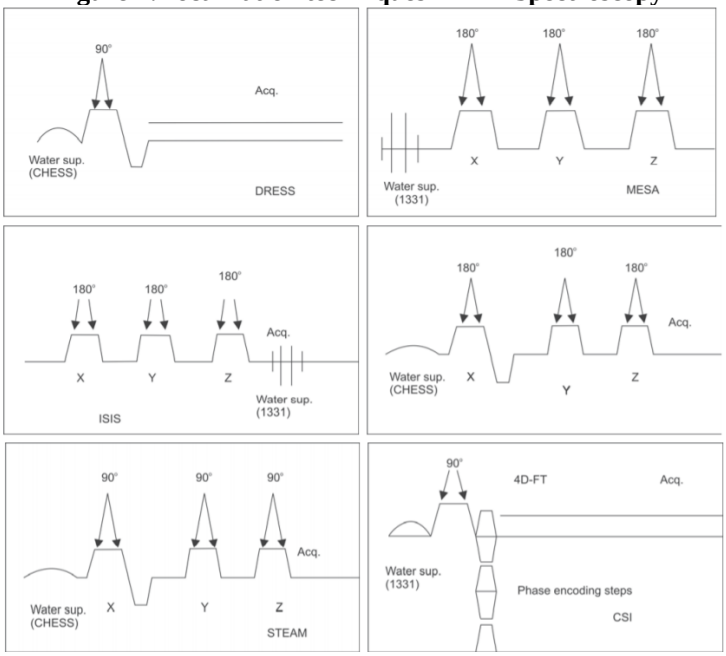

3D Localization methods: There are two effective approaches to localize the MRS signal: (1)Single voxel spectroscopy (SVS). The spatial origin of the signal is constrained by the gradient selection of three orthogonal slices.(2)Multi voxel Spectroscopic imaging (MRS.I.) or chemical shift imaging (CSI) applies spatial phase encoding as in MRI. Thus, the MRS signal from multiple volume elements (voxels) is acquired simultaneously in S.I. (59)

Single voxel vs. multivoxel spectroscopy:

Single voxel studies have excellent localization, field homogeneity, and water suppression based on generating information from a small, well-defined volume in a short time (3-10 min). Multivoxel or CSI has the advantage of obtaining multiple spectra in single data acquisition. CSI takes a long-time for acquisition and is sensitive to motion artifacts. Still, this technique is generally preferred when knowledge of metabolite concentrations' spatial distribution is required within a lesion or organ. Due to R.F. pulses' non-rectangular profile, the spatial origin of the signal in a voxel in CSI does not coincide with the rectangular shape of the voxel. One voxel's signal is contaminated by a signal in other voxels, a phenomenon known as voxel bleeding. This is more pertinent when interpreting the lipid signals in CSI because the lipid signal from the subcutaneous regions is about a thousand times greater than the signal of metabolites. The contribution of lipids to the human brain spectrum to voxel bleeding can be significant. For the same reason, SVS is usually the method of choice when accurate quantification of metabolites is required where voxel bleeding is not significant. (59)

Quantitative Spectroscopy:

Measurement of the concentration of metabolites (quantification) is essential to facilitate the distinction between normal and diseased tissue and for comparison of results from different laboratories. Quantification relies on the calibration of resonance signals with internal or external standards or phantom. The area under a

resonance signal is proportional to the number of nuclei; one can determine the concentration of an unknown peak. Peak width relates to T2 relaxation. Peak width and height can also be used for quantification. (60)

Clinical Applications of MRS of Brain:

Grading of glial tumors: Proton MRS of high-grade gliomas show the significant elevation of Cho, moderate reduction in Cr and reduction in NAA compared with a normal brain. The presence of lactate and lipid resonances correlates with a higher degree of malignancy, as seen in GBM and reflects tumor hypoxia and necrosis. Elevation of Cho reflects increased membrane synthesis and cellularity. (61)

Low-grade gliomas may show marked elevation of myoinositol while higher-grade gliomas show normal or no myoinositol.

Low-grade glioma (LGG) vs. gliomatosis cerebri (G.C.): It may sometimes be challenging to differentiate G.C. from LGG because both tumors present similar morphological characteristics, i.e. infiltration of the large area of brain parenchyma, frequent lack of contrast enhancement and often indistinguishable on brain biopsy. It is observed that patients with G.C. poorly respond to chemotherapy and radiotherapy and have an overall unfavorable prognosis contrary to patients with LGG. The prominent G.C. metabolic features are elevated Cr and NAA levels and a lower level of Cho compared with LGG. Also, there is a clear relationship between the increased levels of Cr and inositol, which may suggest glial activation as a characteristic of G.C. (61)

Reviews:

Hasan et al(62) (2019), conducted a study of 50 patients with brain tumors. Among 50 patients. High-gradegliomas are accounted for 58%, while low-grade gliomas are accounted for 42% based on histopathology. They calculated the relative cerebral blood volume (rCBV) cut off value, more than 1.7 is considered HGG with sensitivity was 96.87%, and specificity was 95.24%. They also calculated the rcbv mean for high-grade glioma, was 3.5 (1.8–6.13), and for a low-grade glioma, the mean was 1.16 (0.5–1.7) (P = 0.0001).They further calculated Cho/Cr value, for high-grade glioma, the mean was 3.5 (1.9–8.75), and for low-grade glioma the mean was 1.6 (1.6–1.8). Cho/NAA, for high-grade glioma, the mean was 5.1 (2–7.5), and for low-grade glioma 1.6 (1.2–1.8). Cho/NAA ratio, at a valueof more than 1.8, viewed HGG with the sensitivity was 100%, and the specificity was 76.2%. Cho/Cr ratio, at a value of 1.8, is considered HGG with the sensitivity was 96.9%, and the specificity was 76.2%. They concluded that the combined use of relative cerebral blood volume and choline/N-acetyl Aspartate increased diagnostic accuracy by 100%.

Radwa K Soliman et al(63) (2018), assess the usefulness of intra-tumour and peri-tumoral relative cerebral blood volume (rCBV) in preoperative glioma grading. Both intra-tumoral and peri-tumoral rCBV of HGG were significantly higher than those of LGG. A cutoff value >2.9 for intra-tumoral rCBV provided sensitivity, specificity, and accuracy of 80%, 100%, and 85.7%, respectivelyto differentiate between HGG and LGG. Additionally, the cutoff value >0.7 for peri-tumoral rCBV provided sensitivity, specificity, and accuracy of 100%, 66.6%, and 90.5%, respectivelyto differentiate between HGG and LGG.

Junfeng Zhang et al(64) (2017), conducted a study on clinical applications of perfusion MRI in Gliomas grading. They concluded that increased rCBV was correlated with more active angiogenesis and aggressive tumour malignancy; it is a potential imaging biomarker for preoperative tumor grading. Considering the leakage effect, several studies introduced correction methods such as preload and algorithm to improve the rCBV accuracy. The corrected rCBV for tumor grading was more accurate than the uncorrected rCBV. The rCBVwas obtained from the region of interest (ROI) based method is inefficient for oligodendroglioma grading, which demonstrates elevated rCBV regardless of tumor grade. rCBVobtained from histogram analysis allows more objective and reliable evaluation for glioma grading than ROI based methods. Increased vascular permeability is another predominant characteristic of tumor vessel, playing an adjuvant role for glioma grading.

EmanA.SH.Geneidiet al(65)(2016), in their study, found that cut off values for rCBV ratio as 2.62 for high-grade glioma and 0.79 for low-grade glioma.

GianvincenzoSparaciaetal(66) (2016), concluded in their study that a relative cerebral blood volume cutoff value of 1.88 for differentiating low-grade gliomas from high-grade gliomas. With sensitivity 100%, specificity 90%, AUC 0.994, PPV 88.9%, NPV 100%, accuracy 94.4% and $P < 0.0001$.

SayedZidan et al(67)(2016), conducted a study in 40 patients who had diagnosed as glioma.19 patients are diagnosed as grade 3 and 24 patients are grade 4. Rcbv was highly significant (p=0.000) in differentiating grade 3 from grade4with cutoff value of 6, with sensitivity 90%, specificity 68.4%, PPV 76%, npv 86.7%.They concluded that MR SPECTROSCOPY ratios of Cho/cr were significant in differentiating grade 3 from grade4.Cho/NAA, NAA/cr were not significant to differentiate two groups.

Nailomeret al(68) (2016), MRS was performed in 22 patients with primary brain tumors. They Calculate metabolite ratios of Choline (Cho)/N-acetyl aspartate (NAA), Cho/Creatine (Cr), Cho+Cr/NAA as well as lipids and lactate (L.L.)/Cr at short and intermediate echo times (T.E.s). Additionally, Myo-inositol (mI)/Cr was calculated at short T.E. Tumors were subdivided into low grades and high grade based on histopathology. They concluded that at intermediate TE, Cho/NAA, Cho+Cr/NAA and Cho/Cr were significantly higher in high-grade tumors than in low-gradetumors. At short TE, Cho/Cr and L.L. /Cr ratios were significantly higher in high-grade tumors than in low-gradetumors. The diagnostic accuracy of metabolite ratios at intermediate T.E. was 86% whereas, at short T.E., the diagnostic accuracy was 75%. A combination of both T.E.s revealed a diagnostic accuracy of 88%. Comparing intermediate T.E. to short T.E., results showed that metabolite ratios' overall diagnostic accuracy was superior atintermediate T.E. to those at short T.E.

FatenMohamed et al(69) (2016), in their study they concluded that Cho/NAA mean value in low-grade glioma was 4.22 ± 2.85;Cho/crmean value was 2.55 ± 1.93 in low-gradeglioma.Cho/NAA mean value in high-grade glioma was 7.12 ± 3.8;Cho/crmean 3.8 ± 2.6. Elevated Cho/NAA and Cho/Cr ratios in tumoral regions of high-gradegliomas (anaplastic glioma and GBM) relative to those seen in low-gradetype. Elevated Lipid and lactate peaks were statistically significant in diagnosing high-grade glioma than in Low-grade gliomas.

Caulo .M et al.(70) conducted a study (2014) in patients with histological confirmed brain gliomas retrospectively. Conventional and advanced M.R. sequences (perfusion-weighted imaging, M.R. spectroscopy, and diffusion-tensor imaging) were performed. Three evaluations were conducted: semi-quantitative (based on traditional and advanced sequences with reported cutoffs), qualitative (exclusively based on conventional M.R. imaging), and quantitative.

For quantitative analysis, four volumes of interest were placed: regions with contrast material enhancement, regions with the highest and lowest signal intensity on T2-weighted images, and regions of most restricted diffusivity.

Significant differences were noted in relative cerebral blood volume (rCBV) values in contrast-enhanced regions (cutoff> 2.59; sensitivity, 80%; specificity, 91%; area under the ROC curve (AUC) = 0.937; P = .0001), areas of lowest signal intensity on T2-weighted images (cutoff >2.45, sensitivity 57%, specificity 97%, AUC 0.852, and P = .0001, respectively), restricted diffusivity regions (cutoff >2.61, sensitivity 54%, specificity 97%,AUC 0.808, and P = .0001, respectively).

Choline/creatine ratio was calculated in regions with the lowest signal intensity on T2-weighted images (cut off >2.07, sensitivity 49%, specificity 88%, AUC 0.685, and P = .0007, respectively). Quantitative analysis showed a higher concordance (p< 0.001) with histological findings than qualitative and semi-quantitativemethods.Rcbv values in contrast-enhanced regions, areas of lowest signal intensity on T2-weighted images, and areas of restricted diffusivity; and choline/creatine ratio in areas with lowest signal intensity on T2-weighted images was used to classify 95% of patients correctly.

M de Fatima Vasco Aragaoet al.(71)(2014) Found that the relative cerebral blood volume mean values were significantly lower in low-grade gliomas (1.4 ± 0.9) compared with the high-grade gliomas (3.3 ± 1.4) P = .0008.They concluded the threshold values ≥1.33 for relative cerebral blood volume provide sensitivity, specificity, positive predictive values, and negative predictive values of 100%, 67%, 87%, and 100%, respectively, for differentiating high-grade gliomas from high-grade gliomas. The lipid-lactate mean values were significantly lower in low-grade gliomas(8.3 ± 11.2) compared with high-grade gliomas (43.3 ± 59.2) and gave the optimal threshold values was ≥7.06 for lipid-lactate to differentiate high-grade from low-grade gliomas.

Aprile, C. Torni, et al.(72)(2012) Conducted a study to evaluate the utility of spectroscopy and perfusion magnetic resonance (M.R.) imaging to differentiate high-grade gliomas from the low-grade tumor. Both for Cho/NAA and rCBV threshold values were obtained using ROC curves. Then diagnostic sensitivity and specificity for high-grade gliomas identification were evaluated for spectroscopic data only (Cho/NAA and lactate presence that was considered a high-grade glioma marker), for perfusion data only (rCBV) and finally for both spectroscopic and perfusion data together. Sensitivity was significantly highest with evaluating both spectroscopic and perfusion data together (89.7%) in comparison with spectroscopy (74.4%) or perfusion (79.4%) alone. Instead, specificity was slightly lower with combined data (91.7%) in comparison with spectroscopy (95.8%) and perfusion (95.8%) alone. They concluded that to characterize high-gradegliomas, it is more useful to evaluate both spectroscopic and perfusion data.

A Di Costanziaet al(73) (2008), conducted their study in high-grade gliomas and calculated rCBV in mass (mean+/-standard deviation (S.D.), 4.3+/-1.2) and margins (4.0+/-1.1) and necrotic areas (0.3+/-0.3).Further calculated in low-grade gliomas, mass (2.0+/-1.5) and margin (2.2+/-1.2) and concluded that rCBV were significantly lower in low-grade glioma and necrotic area than in high-grade gliomas (p<0.001). They also concluded that rCBV intumors showed significantlyhigher thanedema (1.8+/-0.5 vs. 0.5+/-0.2; p<0.001) areas. Three-Tesla PWI helps distinguish necrosis from tumor mass, infiltrating tumor from edema.

PaoloZonari et al(74) (2007), calculated maximum relative cerebral blood volume (rCBV) normalized values between tumor and healthy tissue and maximum Cho/Cr ratio and minimum NAA/Cr ratio in tumor, and calculated lactate and lipid values in the tumor. ROC curves were plotted for parameters with high sensitivity and specificity to identify threshold values to separate high- from a low-grade lesion. Statistically significant differences were found for rCBVtumor/normal tissue ratio and NAA/Cr ratio in tumors and Cho/Cr ratio in tumors between low- and high-grade tumors. They concluded that the best performing single parameter for grading glioma was the normalized rCBV. The ROC curves calculated a high probability for a neoplasm to be a high-grade lesion associated with arCBVtumor/normal tissue ratio of >1.16 and NAA/Cr tumor ratio of <0.44.

BHakyemezet al(75) (2005), conducted a study that involved 33 patients (22 high-grade and 11 low-grade glioma cases). They calculated rCBV and rCBFvalues. In high-grade gliomas, rCBV and rCBF ratios were measured as 6.50±4.29 and 3.32±1.87 (mean±SD). In low-grade gliomas, rCBV and rCBF ratios were 1.69±0.51 and 1.16±0.38, respectively. The rCBV and rCBF ratios for high-grade gliomas were statistically different from those of low-grade gliomas ($p<0.001$). They draw the cutoff value as 1.98 for the rCBV ratio and 1.25 for the rCBF ratio. Perfusion MRI is useful in the preoperative assessment of the histopathological grade of gliomas.

Meng law, Stanely Yang et al(76)(2003). conducted a study in One hundred sixty patients with a primary cerebral glioma underwent conventional M.R. imaging, dynamic contrast-enhanced T2*-weighted perfusion M.R. imaging, and proton M.R. spectroscopy. Gliomas were graded as low or high based on conventional M.R. imaging findings. The rCBV measurements were obtained from regions of maximum perfusion. Metabolite ratios (choline (Cho)/creatine (Cr), Cho/N-acetyl aspartate(NAA), and NAA/Cr) were measured at a TE of 144 ms.

Tumor grade determined with the three methods was then compared with that from histopathology grading. Sensitivity, specificity, PPV, and NPV for determining a high-grade glioma with conventional M.R. imaging were 72.5%, 65.0%, 86.1%, and 44.1%, respectively. They concluded a threshold value of 1.75 for rCBV to provide sensitivity, specificity, PPV, and NPV of 95.0%, 57.5%, 87.0%, and 79.3%, respectively. Threshold values of 1.08 and 1.56 for Cho/Cr and 0.75 and 1.60 for Cho/NAA provided the minimum C2 and C1 errors, respectively, for determining a high-grade glioma. The combination of rCBV, Cho/Cr, and Cho/NAA resulted in sensitivity, specificity, PPV, and NPV of 93.3%, 60.0%, 87.5%, and 75.0%, respectively. Significant differences were noted in the rCBV and Cho/Cr, Cho/NAA, and NAA/Cr ratios between low- and high-grade gliomas ($P < .0001$, .0121, .001, and .0038, respectively).

Shinet al(77) (2002), concluded mean rCBV ratios of 4.91 in high-grade gliomas and 2.00 in low-grade gliomas in 17 patients. They draw the threshold or cutoff value of 2.93 with the use of ROC curve analysis to grade the gliomas.

Sugahara et al(24)(1998), correlated maximal rCBV values with histologically in 30 patients. They concluded the mean values of 7.32, for glioblastomas, 5.84, anaplastic astrocytomas, and low-grade gliomas, 1.26respectively.

Knopp et al(8) (1998), had given mean maximal rCBV values of 5.07 for high-grade gliomas and 1.44 for low-grade gliomas, respectively, in their study.

Lev and Rosen et al(78) (1999), used an rCBV threshold value of 1.5 in discriminating among 32 consecutive patients with glioma. Thirteen (100%) of 13 astrocytomas were correctly categorized as high-grade gliomas. Three of these did not enhance after the administration of contrast material. Of the nine low-grade astrocytomas, seven were correctly classified. The sensitivity and specificity using an rCBV of 1.5 as a threshold value were 100% and 69%, respectively.

Aronen et al(24)(1994), found mean maximal rCBV values of 3.64 and 1.11 in high- and low-grade gliomas, respectively ($n = 19$). They found that the maximum CBV varied from 0.82 to 5.40 in the high-grade group ($n = 13$) and from 1.01 to 1.21 in the low-grade group ($n = 6$). The difference was statistically significant. Maximum CBV was associated with mitotic activity and vascularity, but not with cellular atypia, endothelial proliferation, necrosis, or cellularity.

IV. Materials And Methods

MATERIALS AND METHODS:

The study was conducted in the Radio-diagnosis department, SriVenkateswaraInstitute of Medical Sciences (SVIMS), from March 2019 to July 2020.

INCLUSION CRITERIA:

- All patients with suspected intra cerebralgliomas referred for MRI.
- Patients were willing to enroll in the study after giving informed consent.

EXCLUSION CRITERIA:

- ❖ Patients in whom both PWI and MRS could not be performed.
- ❖ Patients whose histopathological grading on post-operative/biopsy specimens could not be obtained.
- ❖ All tumors/lesions were other than glioma on MRI or histopathology.
- ❖ Patients were not willing to participate in the study.
- ❖ Patients with contraindication for MRI study or intravenous MRI contrast agent.

REGULATORY APPROVALS:

After approval by the Institutional Thesis Protocol Approval Committee and Institutional Ethics Committee, the study was conducted and written informed consent from each patient was obtained before the study. (ANNEXURE1).

DESIGN OF THE STUDY:

A prospective observational study.

STUDY PROCEDURE:

All patients with suspected gliomas referred for MRI, to theDepartment of Radiology; SVIMS were enrolled in the study.

STUDY EQUIPMENT:

PERFUSION WEIGHTED MRI and MR SPECTROSCOPY done on 1.5Tesla SIEMENSMagnetomAera, Germany, using a standard head coils with 48 channels.

Preparation: Patient is asked to remove all metal objects,including keys, coins, wallet, and any cards with magnetic strips, jewellery, hearing aids, and hairpins. Contraindications such as implants, pacemakers, etc. are enquired for MRI study. The patientwas asked to undress and change into a hospital gown. Claustrophobic patients may be accompanied into the scanner room, e.g.,staff member or relative with proper safety screening.

Positioning:

The patient is positioned supine with the head pointing towards the magnet. Head coil is securely around the patient's head.

IMAGING PROTOCOL: All cases were examined using the following protocol:

1. Sagittal T1-WI as a localizer:
*TE = 10-12ms
*TR = 400-600ms
2. Axial and sagittal spin-echo sequences, short TR/TE (T1-weighted images):
*TE = 10-12ms
*TR = 400-600ms
3. Axial, coronal fast spin-echo, long TR/TE (T2-weighted imaging):
*TE = 70-90ms
*TR = 2800-3500ms
4. Axial Fluid Attenuation Inversion Recovery (FLAIR)
TE=110ms
TR=4850ms
5. Post-contrast axial, sagittal and coronal spin-echo sequences, short TR/TE (T1- weighted imaging)
*TE = 10-12ms
*TR = 400-600ms

FOV = 24-18cms in axial images and 30-22cms in coronal images.
Matrix size 192 x 160
Slice thickness = 6mm with 2mm interval, (In all sequences).

Advanced magnetic resonance imaging:

6. Diffusion Weighted Imaging (DWI) with ADC values
TR = 6300ms
TE = 80–100ms,
7. SWI
8. Perfusion weighted imaging
9. Spectroscopy

Perfusion weighted imaging:

Perfusion Weighted Imaging study was performed with a T2-weighted echo-planar spin-echo sequence (TR 1,680, T.E. 30, matrix 128×128, slice thickness 5 mm) with a duration of 84secs.

The following are the steps performed for brain perfusion study on Siemens MR Scanner: We made sure the patient has a good intra-venous line (IV) with a needle gauge of 18 or 20. The patient's IV line is connected to an injector,and the injection rate is set to 5 ml per second. A regular contrast dose of 0.1mmol/kg (Gadodiamide, Omniscan) is used. We made sure the IV line is good and shows no resistance to flow. After starting the routine exam, we inserted the perfusion procedure protocol just before the post-contrast T1.

The perfusion imaging slices had the same positioning, thickness and gap as the axial FLAIR or T2 sequences to facilitate a direct comparison of the perfusion results with other pre- and post-contrast images (Fig. 5). We made sure that both the lesion and cortical white matter are covered. The phase encoding direction is kept anterior-posterior to reduce susceptibility artifacts. After the pre-contrast portion of the brain exam was done, the contrast injection kept ready: we started the scan and injected the contrast at the 8th measurement. The scan has 50-time points (measurements) of ~2 s each resulting in total time just below 2 min.

Figure 5: Slice positioning for perfusion sequence Perfusion sequence

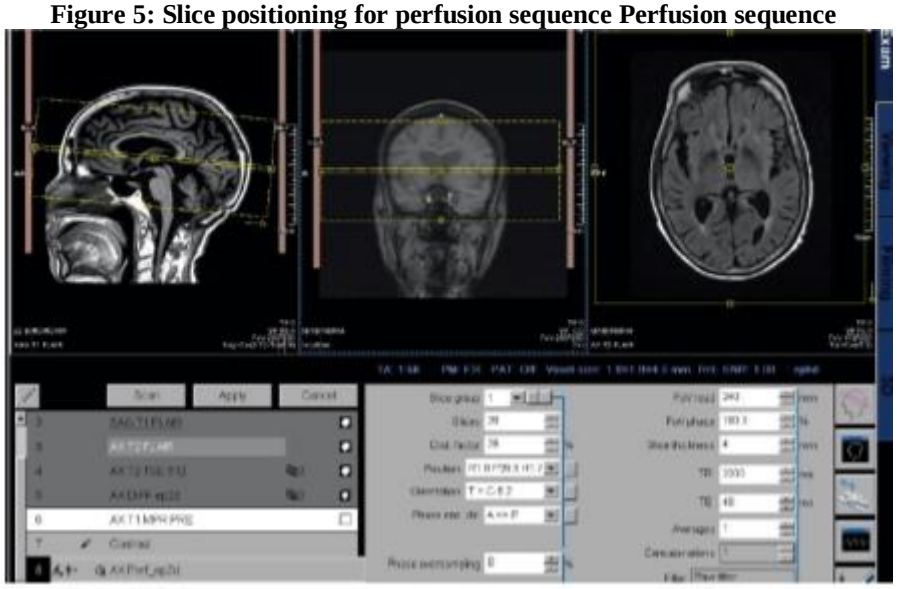

Post-Processing: Post-processing is done on Siemens's workstation (MMWP). After opening the perfusion application, the main perfusion series is extended into the Perfusion Page (Fig. 6).

Figure 6: Opening page of the perfusion application.

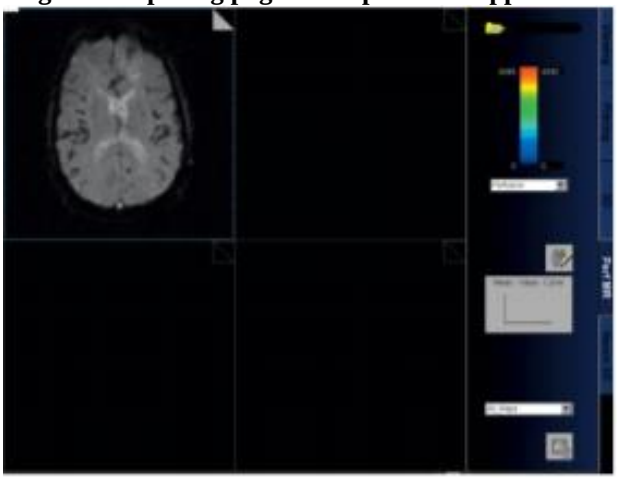

The perfusion series has been dropped and can be seen in the first quadrant (top left). We selected the slice where we can see the area of interest (lesion). An artery on the same slice is identified,and on clicking the arterial input function (AIF) icon, a square appears on the image. The square is placed on the artery (Fig. 7).

Figure 7: Arterial input function (AIF) square is shown on a slice of the perfusion image data.

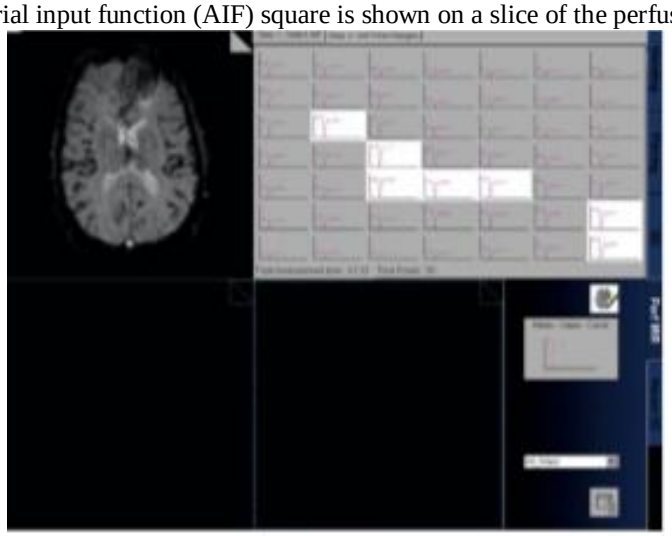

The arterial input function (AIF) square is shown on a slice of the perfusion image data, with the resulting 9x9 pixels time points on the right side. The highlighted region-of-interest (ROI) is used to calculate the AIF.

After selecting AIF, we choose at least four best time graphs, i.e., the ones with a significant signal drop (highlighted squares). Then we set Time Ranges using three lines as shown (Fig. 8). The first one is at the start of the baseline, the second one at the beginning of the drop (Gad entry) and the third one at the peak of the recovery, as shown in Figure 6.

Figure 8: The resulted in AIF, with the three-time points properly shown.

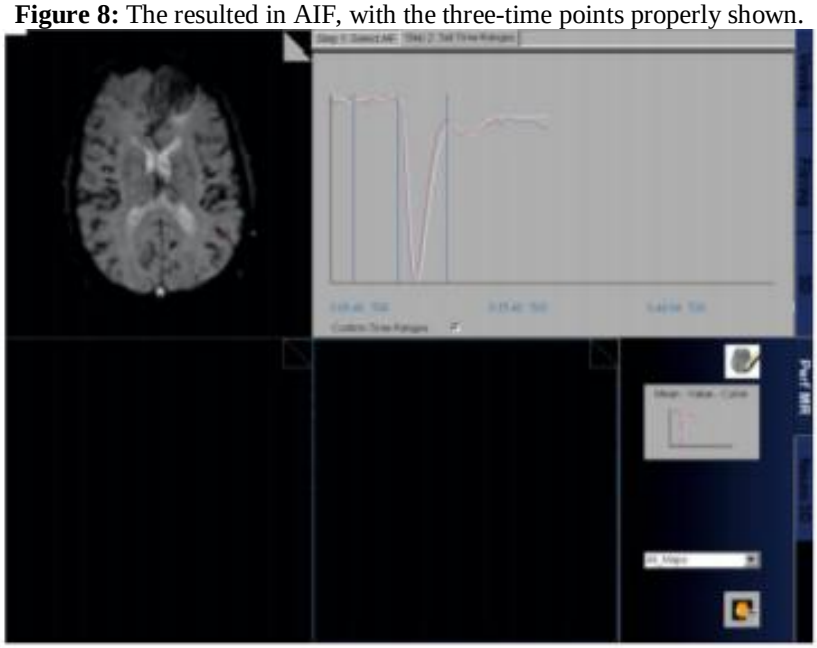

-By clicking on the color calculator icon,the calculation starts,which took about 20 – 30 seconds. Once the calculation is done, the rCBV (relative cerebral blood volume) and rCBF (relative cerebral blood flow) color images are displayed in the screen's 4th quadrant, as shown in figure 9. The third quadrant shows the MTT (mean transit time) and TTP (time-to-peak) maps. Color maps of the cerebral blood volume were generated. The mean of the maximum CBV was obtained by placing a region of interest (ROI) in the peripheral solid areas showing color at the upper end of the color scale. Data is then compared with those of the normal-appearing contralateral white matter.

Figure 9: Shows the perfusion screen, after the calculation is done.

The rCBF and rCBV are displayed in the fourth quadrant (lower right) and the TTP is displayed in 3rd quadrant (lower left).

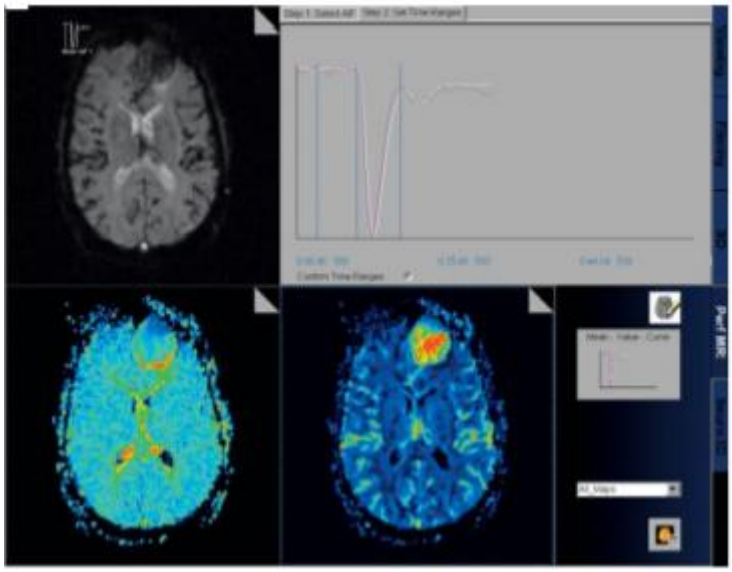

The area under the corrected contrast agent concentration-time curve is proportional to the CBV and does not yield an absolute value. Therefore, it is necessary to express CBV relative to that of a standardreference area, usually the contralateral white matter.

We refer this as relative CBV (rCBV) which is expressed as a ratio. (Ratio = CBV (lesion)/CBV (contra lateral white matter)).

r CBV maps were calculated by post-processing software delivered by M.R. system producer.
r CBV values of enhancing lesions are calculated with ROI placed covering the contrast-enhancing lesion, excluding the necrotic portion.
r CBV normal: ROI is placed on normally appearing corresponding brain parenchyma in the contralateral cerebral hemisphere.

MR SPECTROSCOPY: Spectroscopy Imaging study was performed with a Chemical shift image_se_30 (TR 1500, T.E. 30, matrix 128×128, slice thickness 5 mm) and Chemical shift image_se_135(TR 1890, TE 135, matrix 128×128, slice thickness 5 mm) with a duration of 4minutes.

The Spectroscopy imaging slices had the same positioning, thickness and gap as the axial FLAIR or T2 sequences to facilitate a direct comparison of the Spectroscopy results with other pre- and post-contrast images.Confirm the voxel placement on all three planes and confirm that the voxel is not encroaching onany extraneous tissues.

Post-Processing: Post-processing is done on the Siemens workstation (MMWP). After opening the spectroscopy application, the main spectroscopy series is extended into the spectroscopy Page. The spectroscopy series has been dropped and can be seen in the first quadrant (top left). Voxels were placed within the solid portion of contrast-enhancing lesions. MRS data were evaluated using the L.C. model version. We selected the slice where we can see the area of interest (lesion) then we place a white voxel covering the lesion.

Figure 10:Opening page of MR Spectroscopy

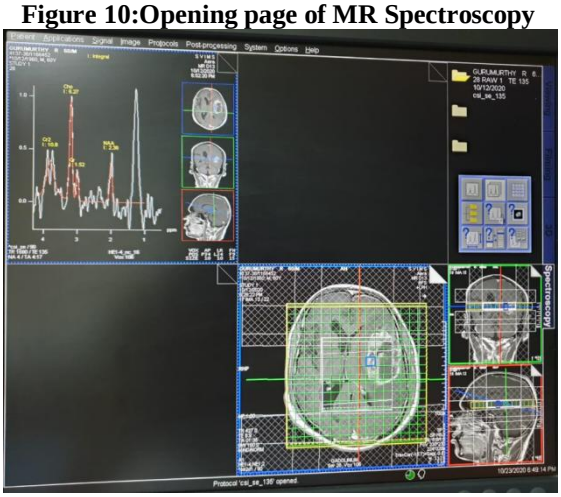

Click the left button on the mouse to select the display parameters. In-display parameters we apply voxel of interest, selected voxel, CSI matrix grid, saturationregions, image text, and scale bar and saturation regions.

Figure 11:Display parameters of MRSpectroscopy

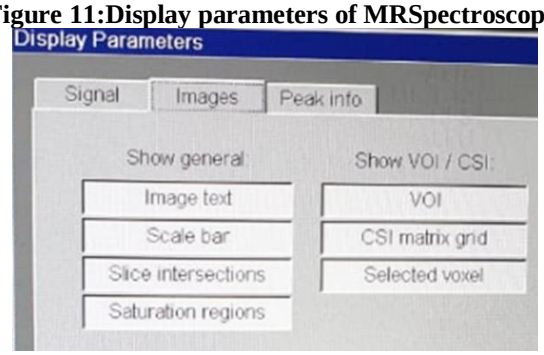

If the area of interest is small click on the post-processing button select modify CSI-FT and adjust interpolation resolution R>>L as 32, A>>P as 32.

Figure 12:shows post-processing and Spatial Fourier Transformation

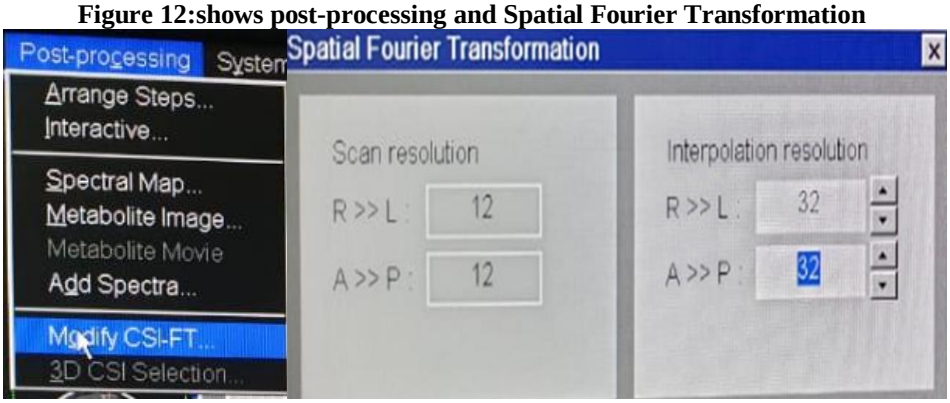

We gave left click on mouse over spectrum quadrant and select result table. Once we select the result table of current spectrum NAA, Cr, Cho values are displayed as ppm.

Figure 13: shows selecting result table

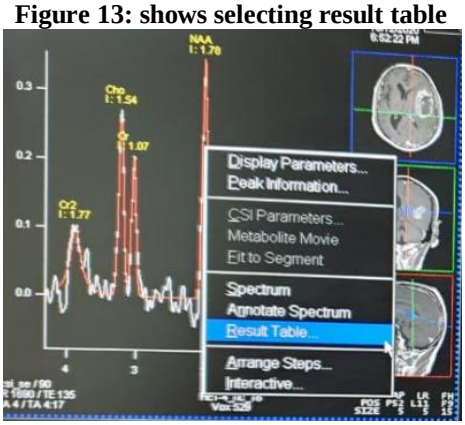

We calculate ratios from this table as follow EX; CHO/Cr ratio we highlight the denominator; it keeps the value as 1.

Figure 14:Result table of MR Spectroscopy

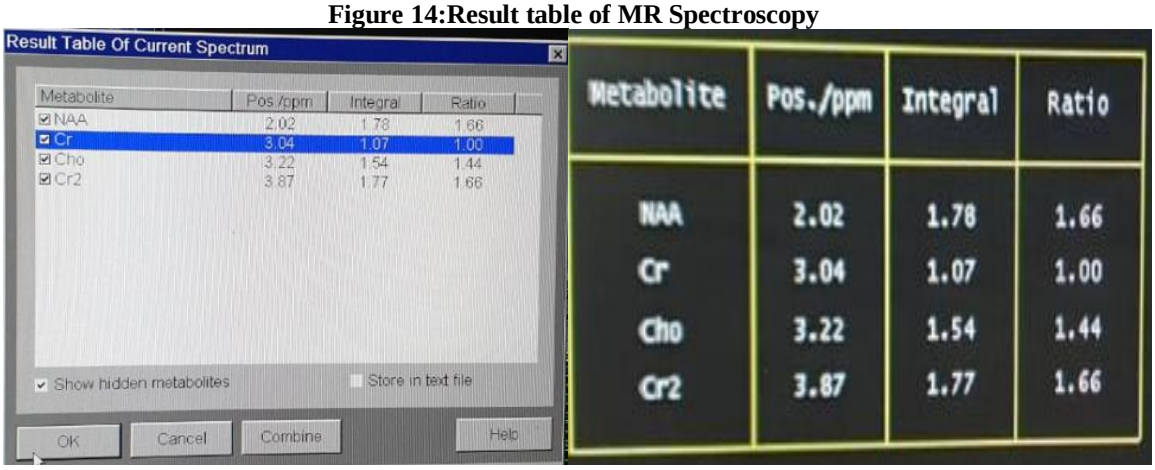

Cho/Cr, Cho/NAA, NAA/Cr ratios were evaluated and tabulated.
Thesis resident initially read PWI and MRSPECTROSCOPY,and upon confirmation by the radiologist enrolled with this study, values were entered into the datasheet.Using Perfusion and spectroscopy findings, preoperative grading of glioma was given. After MRI, patients were followed up till they undergo biopsy/ surgery.

Histopathological grading given by a pathologist who is blinded to MRI findings was obtained and used for analysis. If a patient has both biopsy and post excision histopathology, the latter one was taken into consideration. The study was done according to WHO 2016 classifications (10) as follows. The statistical analysis we reclassified as low-grade gliomas (WHO GRADE1, GRADE2) and high-grade gliomas (WHOGRADE3, GRADE4)

Table 1: DIFFUSE ASTROCYTIC AND OLIGODENDRO GLIAL TUMOURS.

Diffuse astrocytoma,IDH -mutant	II
Anaplastic astrocytoma, IDH -mutant	III
Glioblastoma, IDH -wild	IV
Glioblastoma, IDH -mutant	IV
Diffuse midline glioma	IV
Oligodendro glioma	II
Anaplastic oligodendroglioma	III
OTHER ASTROCYTIC TUMOURS	
Pilocytic Astrocytoma	I
Subependymal giant cell astrocytoma	I

Pleomorphic xanthoastrocytoma	II
Anaplastic Pleomorphicxanthoastrocytoma	III
EPENDYMAL TUMOURS	
Sub ependymoma	I
Myxopapillaryependymoma	I
Ependymoma	II
Ependymoma,RELA fusion-positive	II or III
Anaplastic ependymoma	III
OTHER GLIOMAS	
Angiocentric glioma	I
Choroid glioma of the third ventricle	II

Preoperative MRI grading based on Metabolite ratios of Cho/Cr, Cho/NAA, and NAA/Cr was compared with histopathological grading.
TREATMENT: As appropriate, the patient subsequently underwent surgery, followed by radiotherapy +/_ chemotherapy.

STATISTICAL ANALYSIS:

Data were entered into a computer using computer program Microsoft Excel version 14 (Microsoft Corporation USA).The data was analysed using IBM SPSS statistics software(IBM corp. Released 2019.IBM SPSS statisticsfor windows,version 26.0.Armonk,NY:IBM Corp.) Nominal data were statistically described in terms of percentages, and continuous data were described in terms of mean and standard deviation (±SD) and range. We employed receiver operating characteristic (ROC) curve analysis to assess the performance of a simple diagnostic test designed to correctly grade the tumor as low grade or high-grade using a given rCBV value in relation to defined cutoff. The area under the curve and its statistical significance were calculated. The cut -off point of rCBV values for PWI that would allow differentiation of low-grade glioma and high-grade gliomas were identified. Sensitivity, specificity, positive predictive value, negative predictive value, and accuracy of this diagnostic test were calculated for the retrieved cut-off rCBV value (all values are presented as %). A p-value of less than 0.05 will be considered statistically significant.

Similarly, receiver operating characteristic (ROC) curve analysis was employed to assess the performance of a simple diagnostic test designed to correctly grade the tumor as low -grade or high-grade using a given Cho/cr, Cho/NAA and NAA/cr ratio respectively in relation to the defined cut-off. The area under the curve and its statistical significance were calculated. The cut -off point of Cho/cr, Cho/NAA and NAA/cr ratios respectively that would allow differentiation of low-grade glioma and high-grade gliomas were identified. Sensitivity, specificity, positive predictive value, negative predictive value and accuracy of this diagnostic test were calculated the retrieved cut-off value (all values are presented as %). A p-value of less than 0.05 will be considered statistically significant.

Receiver operating characteristic (ROC) curve analysis was employed to assess the performance of a simple diagnostic test designed to correctly grade the tumor as low -grade or high- grade using rcbv and Cho/cr,CHO/NAA ratios together. The area under the curve and its statistical significance were calculated. sensitivity, specificity, positive predictive value, negative predictive value and accuracy of this combined parameters were calculated. (all values are presented as %).

To determine potentially useful threshold values for rcbv, Cho/cr, Cho/NAA and NAA/cr ratios in differentiating low-grade glioma and high-grade gliomas, threshold values were found that1) minimized the observed number of tumor grade misclassifications(c2 error=fraction of misclassified tumors) and 2)maximized the average of the observed sensitivity and specificity(c1 error).Hence, c1 error=1-(sensitivity=specificity)/2.The Mann-Whitney test was used to compare histologically verified low and high-grade gliomas in terms of rcbv, Cho/cr, Cho/NAA and NAA/cr

V. Observational & Results

RESULTS:

This study included 50 glioma patients .Among 50 patients, 23 patients were males(60%), and 16 patients were females(40%). Age of the patients range from 18 – 75 years, and the mean age was 55.5 years.

Patients were classified into two groups based on their histopathology. The low-grade glioma group included 14 patients (7 male, eight female), (age range 20-68 years, mean age 44 years), and the high-grade

glioma group included 36 patients (16 male, eight female), (age range 18–75 years, mean age 55.5 years. In our study low-gradegliomas constitute about 34%, where as high-grade gliomas are 66%.

Figure 15: Bar diagram showing the age group of patients involved in this study.

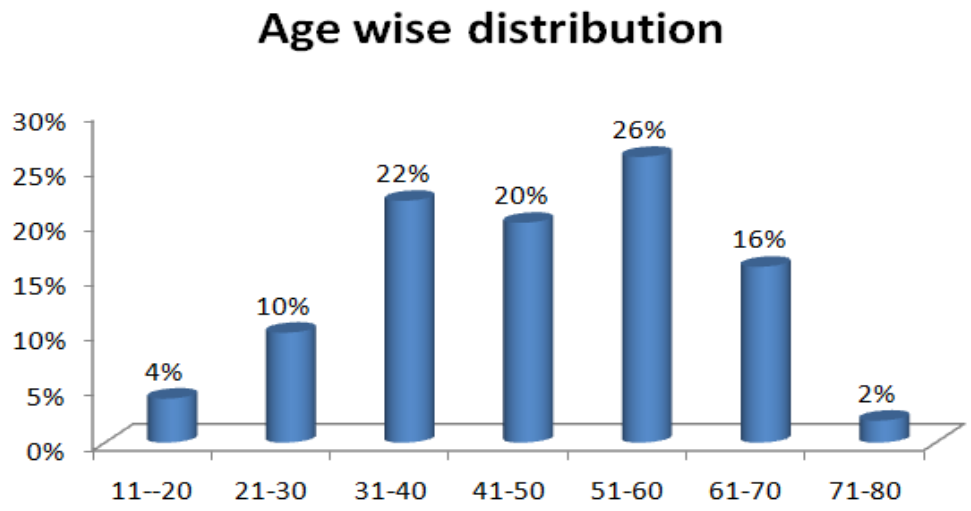

Figure 16: Pie diagram showing the sex distribution of patients involved in this study.

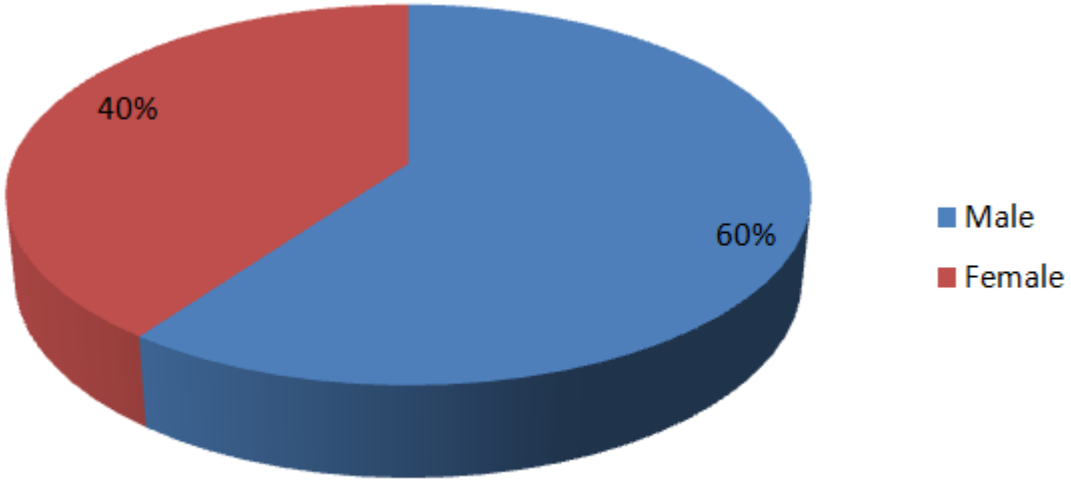

Figure 17: Pie diagram showing the groups of lesions – low-grade glioma and high-grade glioma.

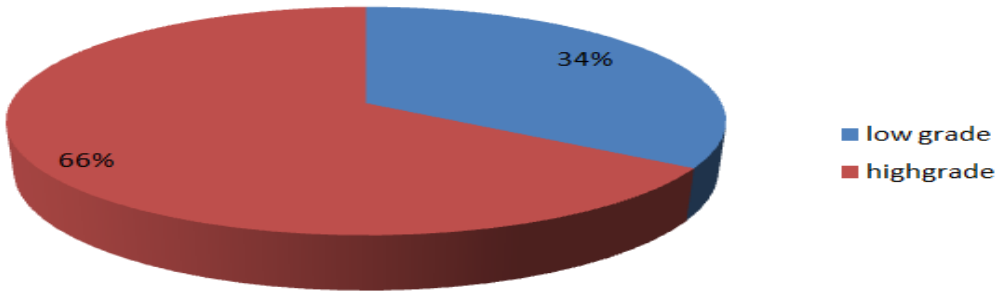

Figure 18: Bar diagram showing histopathological groups of gliomas.

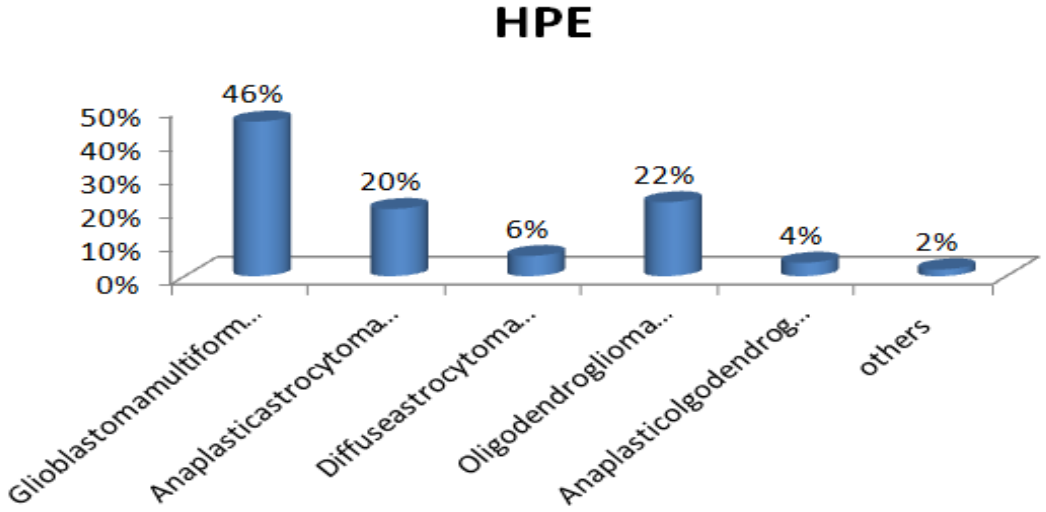

In our study, high-grade gliomas were 66%, whereas low-grade gliomas were 34% according to histopathology. In high-grade glioma group (n=36) most common tumors were glioblastoma multiforme grade 4 (23 patients) followed by anaplastic astrocytoma grade3 (10patients), anaplastic oligodendroglioma grade3 (2 patients) and anaplastic astrooligodendrogliomas (1 patient).In low grade glioma group (n=14) most common tumors were oligodendrogliomas grade2 (11patients) followed by diffuse astrocytomas grade 2(3patients) noted.

Evaluation of discriminatory capability of the PWI method through ROC analysis defined the rCBV value that better allowed a correct differentiation of low-grade from high-grade tumors, retrieving a threshold of 1.54. The ROC curve representing the discriminatory capability of an rCBV value of >1.54 to correctly classify a lesion as high-grade glioma is shown in figure 19. Table 2 demonstrates the corresponding sensitivity, specificity, positive predictive value, negative predictive value and accuracy of this diagnostic test.

Figure 19:ROC curve of rcbv

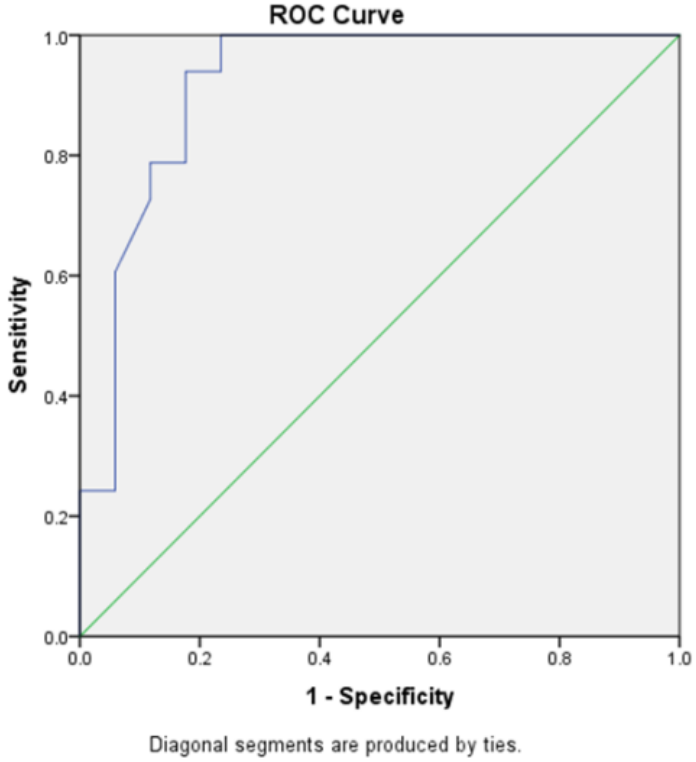

ROC curve representing the discriminatory capability of rCBV in correctly classifying a lesion as high grade using a cutoff point of 1.54. The large area under the curve (0.92) indicates the excellent discriminatory ability of the method.

Table 2: Diagnostic performance of rCBV for the diagnosis of high-grade tumors with a cut-off point of 1.54

Description	rcbv	sensitivity	specificity	PPV	NPV	C2 error	C1 error	accuracy
Minimum c1 error	1.54	84.8	82.4	90.3	73.6	2.5	16.4	84
Minimum c2 error	1.54	84.8	82.4	90.3	73.6	2.5	16.4	84

C2 = the percentage of observed data points misclassified. C1 = 1 − (sensitivity + specificity)/2. This maximizes the average of sensitivity and specificity.

Evaluation of discriminatory capability of the MRS method through ROC analysis defined the Cho/cr ratio that better allowed a correct differentiation of low grade from high-grade tumors, retrieving a threshold of 1.65 .The ROC curve representing the discriminatory capability of an rCBV value of >1.65 to correctly classify a lesion as high-grade glioma is shown in figure 20. Table 3 demonstrates the corresponding sensitivity, specificity, positive predictive value, negative predictive value and accuracy of this diagnostic test.

Figure 20:ROC curve of CHO/CR ratio

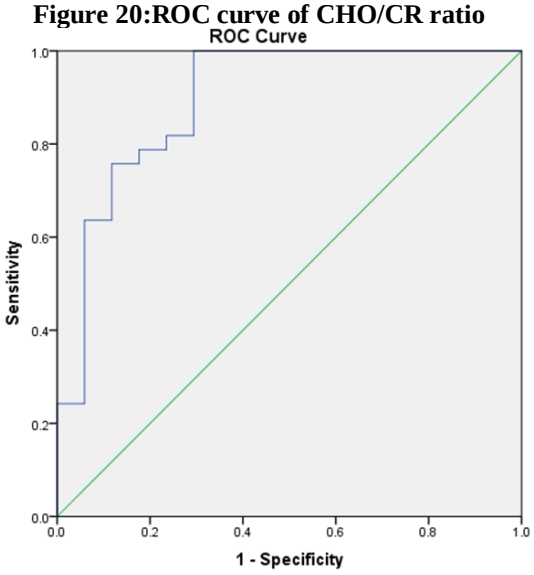

ROC curve represents the Cho/cr ratio's discriminatory capability in correctly classifying a lesion as high grade using a cutoff point of 1.65. The large area under the curve (0.89) indicates the excellent discriminatory ability of the method.

Table 3: Diagnostic performance of Cho/cr ratio for the diagnosis of high-grade tumors with a cut-off point of 1.65

Description	CHO/CR	Sensitivity	Specificity	PPV	NPV	C2	C1	Accuracy
Minimum C1 Error	1.65	100	70.6	86.85	100	3.12	14.7	90
Minimum C2 Error	1.65	100	70.6	86.85	100	3.12	14.7	90

C2 = the percentage of observed data points misclassified. C1 = 1 − (sensitivity + specificity)/2. This maximizes the average of sensitivity and specific it.

Evaluation of discriminatory capability of the MRS method through ROC analysis defined the Cho/NAA ratio that better allowed a correct differentiation of low grade from high-grade tumors, retrieving a threshold of

1.42.The ROC curve representing the discriminatory capability of an rCBV value of >1.42 to correctly classify a lesion as high-grade glioma is shown in figure 21. Table 4 demonstrates the corresponding sensitivity, specificity, positive predictive value, negative predictive value and accuracy of this diagnostic test.

Figure 21:ROC curve of CHO/NAA

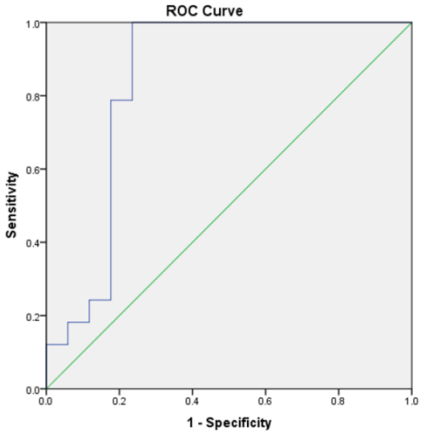

ROC curve represents the Cho/NAA ratio's discriminatory capability in correctly classifying a lesion as high grade using a cutoff point of 1.42. The large area under the curve (0.84) indicates the excellent discriminatory ability of the method.

Table 4: Diagnostic performance of cho/NAA ratio for the diagnosis of high-grade tumors with a cut-off point of 1.42

Description	CHO/NAA	Sensitivity	Specificity	PPV	NPV	C2 Error	C1 Error	Accuracy
Minimum C1 Error	1.42	100	76.5	89.2	100	2.5	11.75	92
Minimum C2 Error	1.42	100	76.5	89.2	100	2.5	11.75	92

Evaluation of discriminatory capability of the MRS method through ROC analysis defined the NAA /cr ratio that better allowed a correct differentiation of low grade from high-grade tumors, retrieving a threshold of 0.04 with minimum c2 error.

The ROC curve representing the discriminatory capability of an NAA/cr ratio of < 0.04 to correctly classify a tumor as high-grade glioma, as shown in figure 22. (minimum c2 error cut –off is best than minimum c1 error) Table 5 demonstrates the corresponding sensitivity, specificity, positive predictive value, negative predictive value and accuracy of this diagnostic test.

Figure 22:ROC curve of NAA/Cr ratio

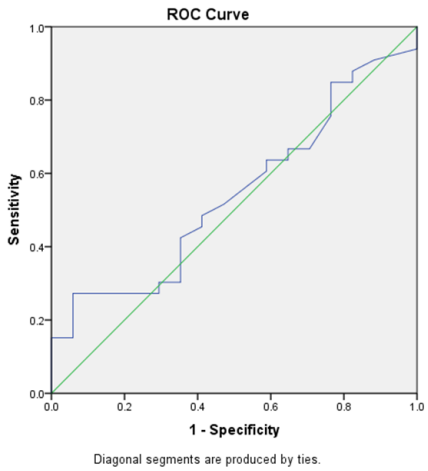

ROC curve represents the NAA/CR ratio's discriminatory capability incorrectly classifying a lesion as high grade using a cut-off point of 0.04The large area under the curve (0.92) indicates the excellent discriminatory ability of the method.

Table 5 : Diagnostic performance of NAA/CR ratio for the diagnosis of high-grade tumors with cut-off point of 1.02 and 0.04

Description	NAA_CR	Sensitivity	Specificity	PPV	NPV	C2 Error	C1 Error	Accuracy
Minimum C1 Error	1.02	27.3	94.1	89.98	40	15.62	39.3	50
Minimum C2 Error	0.04	97	0	65.31	0	11.24	51.5	64

C2 = the percentage of observed data points misclassified. C1 = 1 − (sensitivity + specificity)/2. This maximizes the average sensitivity and specificity

Figure 23:ROC curve of combination(rcbv,Cho/Cr and Cho/NAA ratios)

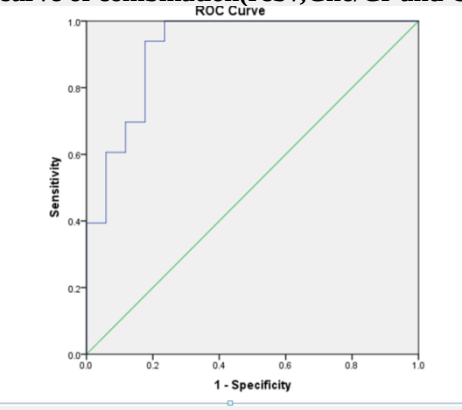

Figure 23:ROC curve representing the discriminatory capability of combined values (rcbv and Cho/Cr, Cho/NAA ratios) in correctly classifying a lesion as high grade the large area under the curve (0.92) indicates the excellent discriminatory ability of the method.

Table 6: Diagnostic performance of combined ratio for the diagnosis of high-grade tumors

Description	Sensitivity	Specificity	PPV	NPV	C2 Error	C1 Error	Accuracy
Minimum C1 Error	100	76.5	89.2	100	2.5	11.75	92
Minimum C2 Error	100	76.5	89.2	100	2.5	11.75	92

C2 = the percentage of observed data points misclassified. C1 = 1 − (sensitivity + specificity)/2. This maximizes the average of sensitivity and specificity.

In the PWI study, the mean rCBV in the enhancing portion of high- grade tumor was 3.38 ± 1.26 (range 4.84). The mean rCBV for low -grade tumor was 1.19± 0. 43range (1.82), which was statistically significant. ($p<0.0001$)

Table 7:Showing mean +/- standard deviation values of rcbv in high-grade and low-grade gliomas.

rcbv	HPE						P value
	High-grade			Low-grade			
	Mean	Standard deviation	Range	Mean	Standard deviation	Range	
	3.38	1.26	4.84	1.19	0.43	1.82	<0.0001

In the MRS study, the mean Cho/cr ratio in the enhancing portion of high-gradetumors was 3.67 ± 1.97 (range 7.62). The mean Cho/cr ratio for low-grade tumors was 1.66± 1.00(range 4.25),which was statistically significant.(p<0.0001)

Table 8: Showing a mean +/- standard deviation values of Cho/cr ratio in high-grade and low-grade gliomas.

	HPE						
	High grade			Low grade			
	Mean	Range	Standard Deviation	Mean	Range	Standard Deviation	P value
Cho/cr	3.67	7.62	1.97	1.66	4.25	1.00	<0.00001

In the MRS study, the mean Cho/NAA ratio in the enhancing portion of the high-grade tumor was 4.23 ± 3.38 (range 16.40). The mean Cho/NAA for low-grade tumors was 1.93± 1.87(range 6.28), which was statistically significant.(p,0.0001

Table 9: Showing a mean +/- standard deviation values of Cho/NAA ratio in high-grade and low-grade gliomas.

	HPE						
	High grade			Low grade			
	Mean	Range	Standard Deviation	Mean	Range	Standard Deviation	P value
Cho/NAA	4.23	16.40	3.38	1.93	6.28	1.87	0.00008

In the MRS study, the mean NAA/cr ratio in the enhancing portion of high-gradetumors was 0.67 ± 0.60 (range 2.45). The mean NAA/cr for low-grade tumors was 0.52± 0.37(range 1.16), which was statistically significant.

Table 10:Showing mean +/- standard deviation values of NAA/CR ratio in high-grade and low-grade gliomas.

	HPE						
	High grade			Low grade			
	Mean	Range	Standard Deviation	Mean	Range	Standard Deviation	P value
NAA/Cr	.67	2.45	.60	.52	1.16	.37	0.63836

IMAGE GALLERY:

Figure24: 23: 35-year-old man with biopsy proved low-grade glioma.

(a) 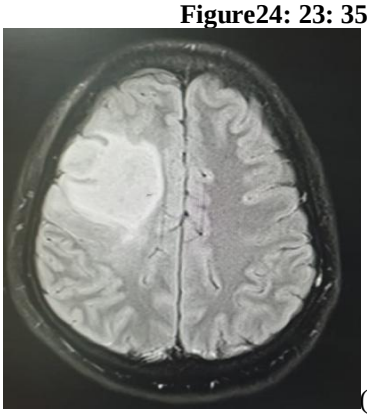 (b) 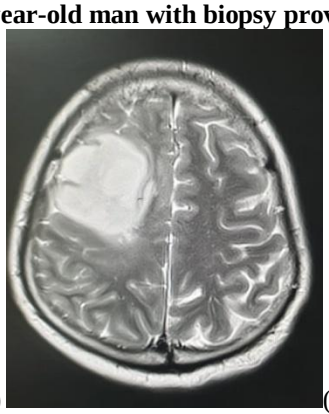 (c) 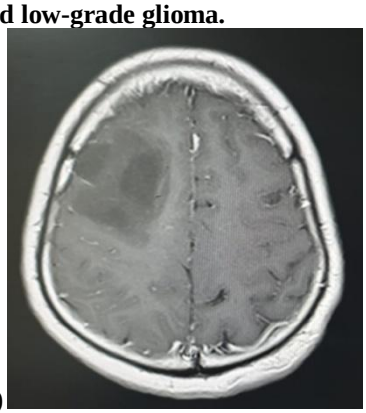

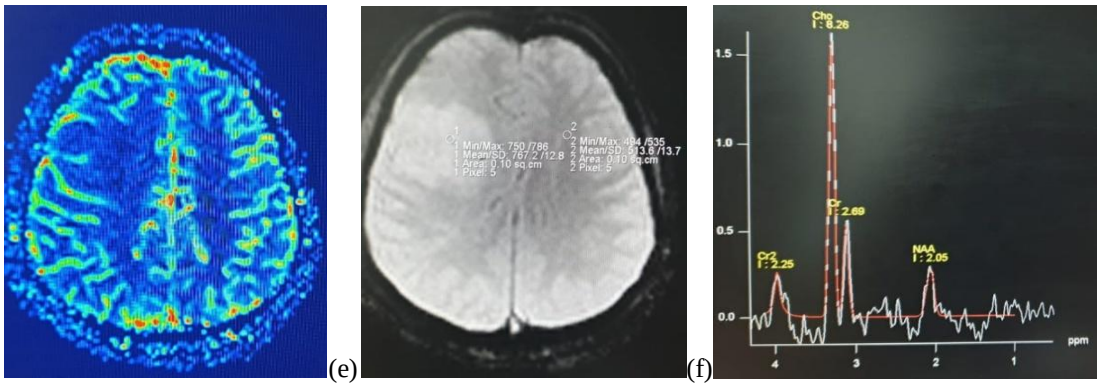

(d) (e) (f)

(a,b): Flair and T2 weighted image demonstrates hyperintense lesion in the right frontal region.
(c):contrast enhanced image demonstrates no enhancement.
(d,e):Gradient-echo axial perfusion MR image with rcbv color overlay map shows a low rcbv of 1.4, in keeping with low-grade glioma.
(f):spectrum from MR spectroscopy with PRESS sequence(135ms) demonstrates elevated choline and slightly decreased NAA with a Cho/cr ratio of 0.9, which is more keeping with low-grade glioma.

Figure 25: 60-year-old woman with biopsy proved high-grade glioma.

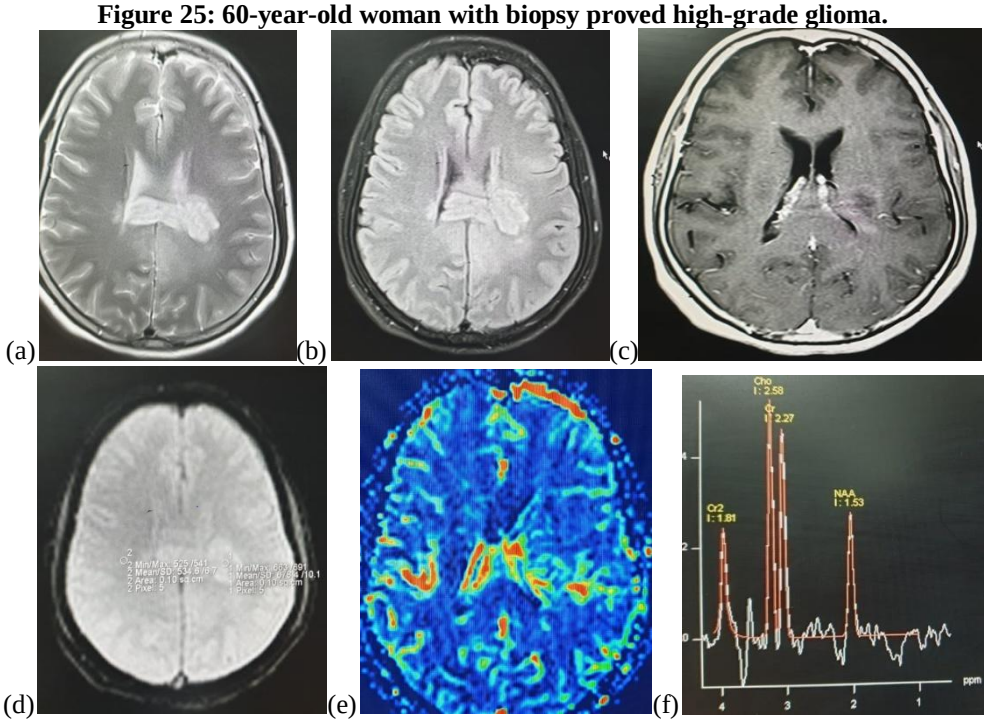

(a) (b) (c)
(d) (e) (f)

(a,b):T2 weighted image and Flair axial image demonstrates hyperintense lesion in spleneum of the corpus callosum.
(c):contrast enhanced image demonstrates minimally enhancing lesion in the splenium of the corpus callosum.
(d,e): Gradient-echo axial perfusion MR image with rcbv color overlay map shows a low rcbv of 2.4, in keeping with high-grade glioma.
(f) :spectrum from MR spectroscopy with PRESS sequence(135 ms) demonstrates markedly elevated choline and decreased NAA with a Cho/NAA ratio of 2.1, as well as lactate peak at 1.3 ppm which is more keeping with high-grade glioma.

VI. Discussion

DISCUSSION:

- Accurate tumor grading has important implications for treatment planning: Patients with an incorrect diagnosis of high-grade glioma will undergo unnecessary adjuvant therapy; on other hand patients with a correct diagnosis of low-grade glioma will be treated conservatively, with concomitant morbidity and mortality.
- The current gold standard of glioma grading is histopathology. It can be inaccurate when biopsy samples are not taken from the most malignant tumor region or when the tumor is not completely resected.

Histopathology grading is often performed on the enhancing portion of the tumor,vessels in the peritumoral region serve as a pathway for tumoral infiltration alongper vascular spaces.The highest vascularity region is corresponding to highest malignancy,also called peritumoral or perienhancing region. (79)

- Radiologic grading of tumors with conventional M.R. imaging is not always accurate. Moller et al,Dean B L et al and Watanable M et al proved that sensitivity in identifying high-grade gliomas with conventional M.R. imaging was 55.1%,83.3%and 72.5% respectively.(80,7,81)
- Perfusion-weighted MRI and M.R. Spectroscopy are advanced M.R. techniques used to add important physiological information to that obtained with conventional MRI. The measurements of these advanced techniques can be used to demonstrate differences between high grade and low-grade gliomas.(82)
- Our study presents a prospective analysis of rCBV and MRS ratios data in 50 patients with intra axial intracerebral gliomas. (36 patients with high-grade gliomas and 14 cases with low-grade gliomas).

Table 11: Showing a comparison of mean +/_ standard deviations PWI values of our study with different studies.

Serial no	High grade glioma	Low grade glioma
Our study	3.38+/_1.26	1.19+/_0.43
Hasan et al(62)	3.5	1.16
Meng law et al(76)	5.18+/_1.67	2.14=/_3.29
Hourani et al(85)	4.9+/_3.1	1.5+/-1.2
Haris et al984)	5.78+/_1.1	2.54=/_0.74
Hakeyemez et al(83)	5.76+/_3.3	1.69+/_0.5
Aronen et al(24)	3.5	1.16

Table 12: Showing a comparison of cut off values and diagnostic performance of PWI in our study with other studies in the literature.

Parameters	Cut off	Sensitivity	Specificity	PPV	npv	Accuracy
Our study	1.5	84.8	82.4	90.3	73.6	84
Hasan et al(62)	1.7	96.8	95.2	96.9	95.2	96
Meng law et al976)	1.75	95	57.5	87	79	90
Hourani et al(85)	1.5	77	91	93	91.7	-
Soliman et al(63)	2.9	80	100	-	-	85.7
Gianvincenzo et al(66)	1.8	100	90	88.9	100	94.4
Caulo.M et al(70)	2.5	80	91	-	-	-

- The study done byHakyemez et al(83), in which a total of 105 patients with varied brain mass lesions were studied (only four cases of infectious lesions, i.e., pyogenic abscesses). They found mean rCBV values of 5.76 ± 3.35 in high-grade gliomas (n= 26), and mean rCBV values of 1.69 ± 0.51 in low-grade gliomas (n= 11). According to this study, high-grade gliomas could be successfully differentiated from low-gradegliomas. (p< 0.0001)
- Haris et al(84), studied 103 patients (77 with neoplastic lesions and 26 patients with infectious lesions).However, the mean rCBV values of high-grade gliomas (5.78 ± 1.11) are not similar to those found in our study (2.38+_ 1.26). This difference in rCBV values might be due to more number of cases in their study compared to our study and due to the different methodologies and the technique.
- Hourani et al (85), these authors found higher mean rCBV values in high-grade tumors (4.9 ± 3.14) in comparison to low-grade tumors (1.5 ± 1.2); In this study, a threshold rCBV value of 1.5 was suggested for differentiating between high grade and low-grade gliomas, with a sensitivity, specificity, positive predictive value and negative predictive value of 77.8%, 91.7%, 93.3% and 91.7%, respectively,which is showing agreement with our study.
- The distinct mean rCBV values found in several different studies may be more useful as qualitative indicators of trends, and should not be taken into an absolute or definitive numeric perspective. The numeric variations may have been affected by multiple factors, including those inherent to the sample (size, heterogeneity and variability of included lesions), subjects (age, immunological status), lesions (type, biological behavior, morphology, dimensions, degree of angiogenesis), scanning protocols, perfusion technique (T1,

gradient-echo or spin-echo sequences, arterial spin labelling), administration or not of the preload of paramagnetic contrast agent, and imaging processing (employed software), among others.

- Several studies have demonstrated a direct correlation between mean rCBV values and histological grading of gliomas, with high-grade gliomas showing higher rCBV values than low-grade gliomas (86-88) which are in accordance, with our study.
- Besides vascular proliferation, cellularity, mitotic activity, nuclear pleomorphism, and necrosis are important criteria in histopathology grading of gliomas. Ki-67 labelling is used in the histological examination as a marker for cellular proliferation. A higher rate of Ki-67–positive cells corresponds to high-grade malignancy in gliomas. Metabolite ratios, in particular Cho levels, have correlated with Ki-67 levels in gliomas (89). M.R. spectroscopic measurements of Cho/Cr and Cho/NAA ratios should be helpful in the grading of gliomas.

Table 13: Showing a comparison of Cho/cr ratio mean values of our study with different studies.

Serial no	High-grade glioma	Low-grade glioma
Our study	3.67+/_1,97	1.66+/-1.00
Hasan et al(62)	3.5	1.6
Meng law et al(76)	2.43+/-3.29	2.14+/-1.67
Faten et al(69)	3.8+/-2.6	2.55+/-1.93

Table14: Showing a comparison of diagnostic performance of cho/cr in our study with other studies.

Parameter	Cut off	Sensitivity	Specificity	PPV	Npv	Accuracy
Our study	1.65	100	70.6	86.8	100	90
Hasan et al(62)	1.8	96.9	76.2	86.1	94.1	73
Meng law et al(76)	1.08	97.5	12.5	77	62.5	-
Caulo .M et al(70)	2	49	88	-	-	89

Table 15: Showing a comparison of Cho/NAA mean values of our study with different studies.

Parameter	High-grade glioma	Low-grade glioma
Our study	4.23+/-3.38	1.93+/_1.98
Hasan et al(62)	5.1	1.6
Meng law et al(76)	3.22=/-3.65	1.96=/_1.43
Faten et al(69)	7.12+/_3.8	4.22+/_2.8

Table 16: Showing a comparison of the diagnostic performance of cho/NAA in our study with other studies.

Parameter	Cut off	Sensitivity	Specificity	PPV	NPV	Accuracy
Our study	1.42	100	76.5	89.2	100	92
Hasan et al(62)	1.8	100	76.2	86.5	100	76.2
Meng law et al(76)	1.60	74.2	62.5	85.6	44.6	-

In our study results, most patients with high-grade gliomas showed elevated Cho/cr, Cho/NAA ratios, in contrast to patients with low-gradegliomas which showed decreased Cho/cr ,Cho/NAA ratios. These results show agreement with previously published studies as Hasan et al and Meng law et al;(62,76)

In our study, NAA/cr ratio mean value for a high grade –gliomas was 0.67+/-0,60, whereas for low-grade gliomas was 0.52+/_0.37. Naa/cr ratios are low in both gliomas, but significantly low in high- grade gliomas. These results were showing agreement with Meng law et al(76) study.(mean for high-grade gliomas1.2+/_0.6,low-grade gliomas 0.9+/_0.7). Cutoff less than 0.04 was highly consistent with high-grade glioma with 97% sensitivity and 64% specificity in our study, which showed agreement with polo zoroni et al.(74)

In our study combination of PWI and MRS demonstrates high sensitivity,specificity and NPV ,compared with previously published study as shown in table:17

Table 17: Showing a comparison of diagnostic performance of the combination of Rcbv, cho/cr,cho/NAA in our study with other studies

Parameters	Sensitivity	Specificity	PPV	NPV	accuracy
Our study	97.7	76.5	89.2	100	92
Meng law et al(76)	93.3	60	87.5	75	-

In our study combination of PWI and MRS ratios demonstrates significantly high sensitivity and NPV. However, specificity was reduced slightly, compared with rcbv alone.

Table 18: Shows comparison of PWI alone and PWI+MRS.

Parameter	Sensitivity	Specificity	PPV	NPV
Rcbv(PWI)	84.8	82.2	90.3	73.6
PWI+MRS	97.7	76.5	89.2	90

In our study combination demonstrates more or less same sensitivity and slightly increased specificity compared to Cho/Cr alone (table) or Cho/NAA alone (table). However, NPV was low with PWI+MRS combination.

Table 19: Shows comparison of Cho/Cr alone and PWI+MRS.

Parameter	Sensitivity	Specificity	PPV	NPV
Cho/Cr	100	70	86.8	100
PWI+MRS	97.7	76.5	89.2	90

Table 20: Shows comparison of Cho/NAA alone and PWI+MRS.

Parameter	Sensitivity	Specificity	PPV	NPV
Cho/NAA	100	76	89	100
PWI+MRS	97.7	76.5	89.2	90

The role of necrosis in glioma grading is important (90). The presence of necrosis is one important distinction between anaplastic astrocytomas and glioblastoma multiforme. In our study, lipid and lactate were found in 42% of low-grade gliomas and in 75% of high-grade gliomas. Our study did not focus on lipids and lactate, formal quantification of these metabolites was not performed. Hence, small amounts of lipids and lactate that may be obscured by baseline noise may not be detected.

VII. Conclusions:

- In conclusion, perfusion-weighted MRI and M.R. Spectroscopy are advanced M.R. techniques used to add important physiological information to that obtained with conventional MRI.
- This study demonstrates that perfusion-weighted (rCBV values of peripheral regions) and Cho/cr ,Cho/NAA and NAA/cr ratios can be used to demonstrate glioma grading preoperatively.
- On perfusion-weighted imaging, high rCBV values in the peripheral portion of the enhancing lesion are strongly suggestive of high-grade glioma. The low rCBV values are highly suggestive of a low-grade glioma etiology.
- The presence of elevation of and Cho/cr, Cho/NAA and NAA/cr ratios above the cut off value strongly suggestive of high-grade glioma.
- The presence of NAA/Cr ratio less than the cut off value strongly suggestive of a high-grade glioma.
- In combination, rCBV measurements and Cho/Cr and Cho/NAA ratios can significantly improve preoperative glioma grading sensitivity and predictive values.
- For these reasons perfusion and M.R. spectroscopy imaging and calculations of rCBV and metabolite values should be performed in all cases of gliomas for radiological grading.

LIMITATIONS:

- The sample size was less in our study, and further validation is required with higher samples.
- The mean rCBV values calculated in our study were based only on analyses of solid enhancing areas without the inclusion of perilesional regions.
- Mean values of Cho/cr, Cho/NAA and NAA/cr are not measured on the normal side.

SUMMARY:

- This study included 50patients in the time frame of March 2019 to July 2020.
- Majority of the patients were males (n=23)
- Age of presentation ranged from 18 – 75 years with a mean age of 55.5 years.
- Based on the final diagnosis, lesions were divided into two groups – the high-grade glioma group (n=36) and low-gradeglioma group (n=14).
- MRS values were calculated from the enhancing portion of the lesion, and rCBVvalues were calculated from the enhancing solid component showing color at the upper end of the scale.
- In the perfusion study, the mean rCBV in the high-grade glioma lesions was 2.38±1.26 (range 4.84). The mean rCBV for low grade glioma lesions was 1.19±0.43 (range1.82). The difference in rCBV values between the high-grade glioma lesions and low-grade glioma lesions was statistically significant ($p < 0.001$).
- In MRS, on quantitative assessment, the mean Cho/cr value of the high-grade gliomas were3.67 ± 1.97 while 1.66 ± 1 for the low-grade gliomas, which was statistically significant ($p < 0.01$).
- On the other hand, the mean value of Cho/NAA, NAA/ cr ratios were 4.23+/_3.38 n,0.67+/_2.45 for high-grade gliomas, respectively, while the mean value of Cho/NAA, NAA/ cr ratios were1.93/_1.87 and 0.52/-0.37 for low-grade gliomas respectively.
- In PWI cut off of rcbv value was 1.54; in MRS cut off Cho/cr, Cho/NAA, NAA/cr ratios were 1.65, 1.42.0.04 respectively to differentiate high-grade gliomas from low-grade gliomas.
- Cut-off of NAA/Cr was 0.04.NAA/ Cr ratio less than 0.04 strongly suggestive of high-grade glioma.

BIBLIOGRAPHY

REFERENCES:;

[1]. Ostrom QT, Gittleman H, Liao P, Rouse C, Chen Y, Dowling J, Wolinsky Y. CBTRUS statistical report: primary brain and central nervous system tumours diagnosed in the United States in 2007- 2011. NeuroOncol 2014; 16 (4): iv1-63.
[2]. Wen PY, Reardon DA. progress in glioma diagnosis, classification and treatment. Nature Reviews Neurology. 2016; 12(2): 69–70.
[3]. Weller M, van den Bent M, Hopkins K, Tonn JC, Stupp R, Falini A et al.EANO guideline for the diagnosis and treatment of anaplastic gliomas and glioblastoma. Lancet Oncology.2014;15(9):e395–e403.
[4]. Smits M. Imaging of oligodendroglioma. Br J Radiol 2016;89:1060.
[5]. Scott JN, Brasher PM, Sevick RJ, Rewcastle NB, Forsyth PA. Forsyth. How often are nonenhancingsupratentorial gliomas malignant? A population study. Neurology. 2002;59:947–949.
[6]. Whittle R. The dilemma of low grade glioma. J NeurolNeurosurg Psychiatry. 2004;75(2): ii31–ii36.
[7]. Dean BL, Drayer BP, Bird CR, Flom RA, Hodak JA, Coons SW et al. Gliomas: classification with MR imaging. Radiology. 1990;174:411–415.
[8]. Knopp EA, Cha S, Johnson G, Mazumder A, Golfinos JG, Zagzag D et al. Glial neoplasms: dynamic contrast-enhanced T2*-weighted MR imaging. Radiology. 1999;211: 791–798,
[9]. Möller-Hartmann W, Herminghaus S, Krings T, Marquardt G, Lanfermann H, Pilatus U et al. Clinical application of proton magnetic resonance spectroscopy in the diagnosis of intracranial mass lesions. Neuroradiology. 2002;44:371– 38.
[10]. Bielle F. Building diagnoses with four layers: WHO 2016 classification of CNS tumors. Rev Neurol (Paris). 2016;172(4-5):253-5.
[11]. Gittleman HR, Ostrom QT, Rouse CD, Dowling JA, De Blank PM, Kruchko CA et al. Trends in central nervous system tumor incidence relative to other common cancers in adults, adolescents, and children in the United States, 2000 to 2010. Cancer. 2015;121(1):102-12.
[12]. Condello S, Nwani NG, Matei D et al. The hunt for elusive cancer stem cells. Oncotarget. 2017;8(24):38076-38077.
[13]. Perry A, Wesseling P. Histologic classification of gliomas. Handb Clin Neurol. 2016;134:71-95.
[14]. Ballester LY, Huse JT, Tang G, Fuller GN. Molecular classification of adult diffuse gliomas: conflicting IDH1/IDH2, ATRX, and 1p/19q results. Human pathology. 2017;69:15-22.
[15]. Capdevila C. Glioblastoma multiforme and adult neurogenesis in the ventricular-subventricular zone: a review. J Cell Physiol. 232(7):1596-1601, 2017.
[16]. Karsy M, Guan J, Cohen AL, Jensen RL, Colman H. New molecular considerations for glioma: IDH, ATRX, BRAF, TERT, H3 K27M. CurrNeurolNeurosci Rep. 2017;17(2):19.
[17]. Komori T. Pathology of oligodendroglia: an overview. Neuropathology.2017;37(5):465-474.
[18]. Bi Z, Ren X, Zhang J, Jia W. Clinical, radiological, and pathological features in 43 cases of intracranial subependymoma. J Neurosurg. 2015;122(1):49-60.
[19]. Hardee ME, Zagzag D. Mechanisms of glioma-associated neovascularization. Am J Pathol.2012;181(4):1126–41.
[20]. Jain RK, Di Tomaso E, Duda DG, Loeffler JS, Sorensen AG, Batchelor TT. Angiogenesis in brain tumours. Nature Rev Neurosci. 2007;8(8):610–622.
[21]. Wolburg H, Noell S, Fallier-Becker P, Mack AF, Wolburg-Buchholz K. The disturbed blood-brain barrier in human glioblastoma. Mol Aspect Med. 2012;33(5):579–589.
[22]. Padera TP, Stoll BR, Tooredman JB, Capen D, di Tomaso E, Jain RK. Cancer cells compress intratumour vessels. Nature. 2004;427:695.
[23]. Vartanian A, Singh SK, Agnihotri S, Jalali S, Burrell K, Aldape KD. GBM's multifaceted landscape: highlighting regional and microenvironmental heterogeneity. Neuro-Oncology. 2014;16(9):1167–75.
[24]. Aronen HJ, Gazit IE, Louis DN, Buchbinder BR, Pardo FS, Weisskoff RM et al. Cerebral blood volume maps of gliomas: comparison with tumor grade and histologic findings. Radiology. 1994;191:41–51.
[25]. Sugahara T, Korogi Y, Kochi M, Ikushima I, Hirai T, Okuda T et al. Correlation of MR imaging–determined cerebral blood volume maps with histologic and angiographic determination of vascularity of gliomas. Am J Roentgenol. 1998;171:1479–86.
[26]. Folkman J. Seminars in medicine of the Beth Israel Hospital, Boston: clinical applications of research on angiogenesis. N Engl J Med. 1995;333:1757–63.

[27]. O'Reilly MS, Holmgren L, Shing Y, Chen C, Rosenthal RA, Cao Y et al. Angiostatin: a circulating endothelial cell inhibitor that suppresses angiogenesis and tumor growth. Cold Spring HarbSymp Quant Biol. 1994;59:471–82.
[28]. O'Reilly MS, Boehm T, Shing Y, Fukai N, Vasios G, Lane WS et al. Endostatin: an endogenous inhibitor of angiogenesis and tumor growth. Cell. 1997;88:277–85.
[29]. Kirsch M, Strasser J, Allende R, Bello L, Zhang J, Black PM. Angiostatin suppresses malignant glioma growth in vivo. Cancer Res. 1998;58:4654–9.
[30]. Wu Z, O'Reilly MS, Folkman J, Shing Y. Suppression of tumor growth with recombinant murine angiostatin. BiochemBiophys Res Commun. 1997;236:651–4. .
[31]. Rosen BR, Belliveau JW, Vevea JM, Brady TJ. Perfusion imaging with NMR contrast agents. MagnReson Med. 1990;14:249–265.
[32]. Walker C, Baborie A, Crooks D, Wilkins S, Jenkinson MD. Biology, genetics and imaging of glial cell tumours. Br J Radiol. 2011;84:S90–106.
[33]. Law M, Yang S, Wang H, Babb JS, Johnson G, Cha S et al. Glioma grading: Sensitivity, specificity, and predictive values of perfusion MR imaging and proton MR spectroscopic imaging compared with conventional MR imaging. AJNR Am J Neuroradiol. 2003;24:1989– 1998.
[34]. Hu LS, Eschbacher JM, Heiserman JE, Dueck AC, Shapiro WR, Liu S et al. Reevaluating the imaging definition of tumor progression: Perfusion MRI quantifies recurrent glioblastoma tumor fraction, pseudoprogression, and radiation necrosis to predict survival. Neuro Oncol. 2012;14:919–930.
[35]. Essig M, Shiroishi MS, Nguyen TB, Saake M, Provenzale JM, Enterline D et al. Perfusion MRI: The five most frequently asked technical questions. AJR Am J Roentgenol. 2013;200:24–34.
[36]. Bedekar D, Jensen T, Schmainda KM. Standardization of relative cerebral blood volume (rCBV) image maps for ease of both inter- and intrapatient comparisons. MagnReson Med. 2010;64:907–913.
[37]. Paulson ES, Schmainda KM. Comparison of dynamic susceptibility-weighted contrast-enhanced MR methods: Recommendations for measuring relative cerebral blood volume in brain tumors. Radiology. 2008;249:601–613.
[38]. Quarles CC, Gochberg DF, Gore JC, Yankeelov TE. A theoretical framework to model DSCMRI data acquired in the presence of contrast agent extravasation. Phys Med Biol. 2009;54:5749–5766.
[39]. Willats L, Calamante F. The 39 steps: Evading error and deciphering the secrets for accurate dynamic susceptibility contrast MRI. NMR Biomed. 2013;26:913–931.
[40]. Gahramanov S, Muldoon LL, Li X, Neuwelt EA. Improved perfusion MR imaging assessment of intracerebral tumor blood volume and antiangiogenic therapy efficacy in a rat model with Ferumoxytol. Radiology. 2011;261:796–804.
[41]. Boxerman JL, Schmainda KM, Weisskoff RM. Relative cerebral blood volume maps corrected for contrast agent extravasation significantly correlate with glioma tumor grade, whereas uncorrected maps do not. AJNR Am J Neuroradiol. 2006;27:859–867.
[42]. Speck O, Chang L, DeSilva NM, Ernst T. Perfusion MRI of the human brain with dynamic susceptibility contrast: Gradient-echo versus spin-echo techniques. J MagnResonImaging. 2000;12:381–387. 70
[43]. Schmiedeskamp H, Andre JB, Straka M, Christen T, Nagpal S, Recht L et al. Simultaneous perfusion and permeability measurements using combined spin- and gradient-echo MRI. J Cereb Blood Flow Metab. 2013;33:732–743.
[44]. Schmiedeskamp H, Straka M, Newbould RD, Zaharchuk G, Andre JB, Olivot JM et al. Combined spin- and gradient-echo perfusion-weighted imaging. MagnReson Med. 2012;68:30–40.
[45]. Alvarez-Linera J. 3T MRI: Advances in brain imaging. Eur J Radiol. 2008;67:415– 426.
[46]. Liu HL, Wu YY, Yang WS, Chen CF, Lim KE, Hsu YY. Is Weisskoff model valid for the correction of contrast agent extravasation with combined T-1 and T-2* effects in dynamic susceptibility contrast MRI? Med Phys. 2011;38:802–809.
[47]. Mauz N, Krainik A, Tropres I, Lamalle L, Sellier E, Eker O. Perfusion magnetic resonance imaging: Comparison of semiologic characteristics in first-pass perfusion of brain tumors at 1.5and 3 tesla. J Neuroradiol. 2012;39:308-16.
[48]. Cousins JP. Clinical MR spectroscopy Fundamentals, current applications and future potential. AJR. 1995;164:1337-47.
[49]. Bolinger L, Insko EK. Spectroscopy: Basic principles and techniques. In: Edelman RR, Hesselink JR, Zlatkin MB. (Eds): Body MRI. WB Saunders, Philadelphia 1996;353-79.
[50]. Matson GB, Weiner MW. Spectroscopy in Magnetic Resonance Imaging. Stark DD, Bradley WG (Ed): Mosby, St Louis 1999;181-211.
[51]. Skoch A, Jiru F, Bunke J. Spectroscopic imaging: basic principles. Eur J Radiol. 2008;67:230-39.
[52]. Soares DP, Law M. Magnetic resonance spectroscopy of the brain: review of metabolites and clinical applications; Clin Radiol. 2009;64:12-21.
[53]. Birken DL, Oldendorf WH. NAA: A literature review of compound prominent of proton spectroscopy of brain. NeurosciBiobehv Rev. 1989;13:23-31.
[54]. Rothman DL, Arias MF, Shulman GI. A pulse sequence for simplifying hydrogen NMR spectra of biological tissues. J MagnReson. 1984;60:430-34.
[55]. Behar KL, Rothman DL, Spencer DDPetroff OA. Analysis of macromolecule resonances in 1H-MRS spectra of human brain. Mag Reson Med. 1994;32:294-98.
[56]. Brateman L. Chemical shift imaging: a review, Am J Radiol. 1986;146:971.
[57]. Usenius JP, Kauppinen RA, Vainio PA, Hernesniemi JA, Vapalahti MP, Paljärvi LA et al. Quantitative metabolite patterns of human brain tumors: Detection by 1 H-NMR spectroscopy in vivo and in vitro. J Comput Assist Tomogr. 1994;18:705.
[58]. Oberhaensli R, Bore P, Rampling R, Hilton-Jones D, Hands L, Radda G. Biochemical investigation of human tumors in vivo with phosphorus-31 magnetic resonance spectroscopy. Lancet. 1986;5:8.
[59]. Fulham MJ, Bizzi A, Dietz MJ, Shih HH, Raman R, Sobering GS et al. Mapping of brain tumor metabolites with proton MR spectroscopic imaging: Clinical relevance, Radiology 1992;185:675.
[60]. Kuesel AC, Sutherland GR, Halliday W,Smith IC. 1 H- MRS of highgradeastrocytomas: Mobile lipid accumulation in necrotic tissue, NMR Biomed. 1994;7:149.
[61]. Smith JK, Castillo M, Kwock L. MR spectroscopy of brain tumors. MagnReson Imaging Clin N Am. 2003;11:415.

[62]. Hasan AM, Hasan AK, Megally HI, Khallaf M, Haseib A. The combined role of MR spectroscopy and perfusion imaging in preoperative differentiation between high- and low-grade gliomas. EJRNM. 2019;50:1-9.
[63]. Soliman RK, Gamal SA, Essa AH, Othman MH. Preoperative Grading of Glioma Using Dynamic Susceptibility Contrast MRI: Relative Cerebral BloodVolume Analysis of Intra-tumoural and Peri-tumoural Tissue. Clin NeurolNeurosurg. 2018;167:86-92.
[64]. Zhang J, Liu H, Tong H, Wang S, Yang Y, Liu G. Clinical Applications of Contrast-Enhanced Perfusion MRI Techniques in Gliomas: Recent Advances and Current Challenges. Contrast Media Mol Imaging. 2017;2017:7064120.
[65]. lEmanA.SH.Geneidi[a]LobnaA.Habib[a]NivineA.Chalabi[a]MohamedH.Haschim[b] Potential role of quantitative MRI assessment in differentiating high from low-grade gliomasejrnm;2015;005:11
[66]. Sparacia G, Gadde JA, Iaia A, Sparacia B, Midiri M. Usefulness of quantitative peritumoural perfusion and proton spectroscopic magnetic resonance imaging evaluation in differentiating brain gliomas from solitary brain metastases. 2016;29:160–167
[67]. Zidan S, Tantawy HI, Makia MA.High grade gliomas;The role of dynamic contrast-enhanced susceptibility-weighted perfusion MRI and Proton MR Spectroscopic imaging in differentiating grade 3 from grade 4. EJRNM. 2016;47(4):1565-73
[68]. Naser RK, Hassan AA, Shabana AM, Omar NN. Role of magnetic resonance spectroscopy in grading of primary brain tumors. EJRNM. 2016;47:577-84.
[69]. Fawzy FM, Almassry HN, Ismail AM. Preoperative glioma grading by MR diffusion and MR spectroscopic imaging. EJRNM;2016;47(4):1539-48.
[70]. Caulo M, Panara V, Tortora D, Mattei PA, Briganti C, Pravatà E et al. Data-driven grading of brain gliomas: a multiparametric MR imaging study.Radiology. 2014;272(2):494-503.
[71]. Aragao MD, Law M, De Almeida DB, Fatterpekar G, Delman B, Bader AS et al. Comparison of perfusion, diffusion, and MR spectroscopy between low-grade enhancing pilocytic astrocytomas and high-grade astrocytomas. Epub. 2014;35(8):1495-502.
[72]. Aprile I, Torni C, Fiaschini P, Muti M. High-Grade Cerebral Glioma Characterization: Usefulness of MR Spectroscopy and Perfusion Imaging Associated EvaluationNeuroradiol J.2012;25:57-66.
[73]. Di Costanzo A, Pollice S, Trojsi F, Giannatempo GM, Popolizio T, Canalis Let al.Role of perfusion-weighted imaging at 3 Tesla in the assessment of malignancy of cerebral gliomas. La radiologia medica. 2008;113(1):134-43.
[74]. Zonari P, Baraldi P, Crisi G.Multimodal MRI in the characterization of glial neoplasms: the combined role of single-voxel MR spectroscopy, diffusion imaging and echo-planar perfusion imaging. Neuroradiology. 2007;49(10):795–803.
[75]. Hakyemez B, Erdogan C, Ercan I, Ergin N, Uysal S, Atahan S.High-grade and low-grade gliomas: differentiation by using perfusion MR imaging.Clinical Radiology;2005;60(4): 493-502.
[76]. Meng Law, Stanley Yang, Hao Wang, James S. Babb, Glyn Johnson, Soonmee Cha, Edmond A. Knopp and David Zagzag. Glioma Grading: Sensitivity, Specificity, and Predictive Values of Perfusion MR Imaging and Proton MR Spectroscopic Imaging Compared with Conventional MR Imaging.Am J Neuroradiol. 2003;24 (10): 1989-98.
[77]. Shin JH, Lee HK, Kwun BD, Kim JS, Kang W, Choi CG et al. Using relative cerebral blood flow and volume to evaluate the histopathologic grade of cerebral gliomas: preliminary results. Am J Roentgenol. 2002;179:783–78
[78]. Lev MH, Rosen BR. Clinical applications of intracranial perfusion MR imaging. Neuroimaging Clin N Am. 1999;9:309–31.
[79]. Cha S, Knopp EA, Johnson G, Wetzel SG, Litt AW, Zagzag D et al. Intracranial mass lesions: dynamic contrast-enhanced susceptibility-weighted echo-planar perfusion MR imaging. Radiology. 2002;223:11–29.
[80]. Möller-Hartmann W, Herminghaus S, Krings T, Marquardt G, Lanfermann H, Pilatus U et al. Clinical application of proton magnetic resonance spectroscopy in the diagnosis of intracranial mass lesions. Neuroradiology 2002;44:371– 381
[81]. Watanabe M, Tanaka R, Takeda N. Magnetic resonance imaging and histopathology of cerebral gliomas. Neuroradiology. 1992;34: 463–469
[82]. Kondziolka D, Lunsford LD, Martinez AJ. Unreliability of contemporary neurodiagnostic imaging in evaluating suspected adult supratentorial (low-grade) astrocytoma. J Neurosurg. 1993;79:533–536.
[83]. Hakyemez B, Erdogan C, Bolca N, Yildirim N, Gokalp G, Parlak M et al. Evaluation of different cerebral mass lesions by perfusion-weighted MR imaging. J MagnReson Imaging. 2006;24:817–824.
[84]. Haris M, Gupta RK, Singh A, Husain N, Husain M, Pandey CM et al. Differentiation of infective from neoplastic brain lesions by dynamic contrast-enhanced MRI. Neuroradiology. 2008;50:531–540.
[85]. Hourani R, Brant LJ, Rizk T, Weingart JD, Barker PB, Horská A. Can proton MR spectroscopic and perfusion imaging differentiate between neoplastic and nonneoplastic brain lesions in adults? AJNR Am J Neuroradiol. 2008;29: 366–372.
[86]. Rollin N, Guyotat J, Streichenberger N, Honnorat J, Minh VA, Cotton F et al. Clinical relevance of diffusion and perfusion magnetic resonance imaging in assessing intraaxial brain tumors. Neuroradiology.2006;48:150-9.
[87]. Toh CH, Wei KC, Ng SH, Wan YL, Lin CP, Castillo M. Differentiation of brain abscesses from necrotic glioblastoma and cystic metastatic brain tumours with diffusion tensor imaging. AJNR. 2011;32:1646–51.
[88]. Chiang IC, Hsieh TJ, Chiu ML, Liu GC, Kuo YT, Lin WC et al. Distinction between pyogenic brain abscess and necrotic brain tumors using 3-tesla MR spectroscopy, diffusion and perfusion imaging. Br J Radiol. 2009;82:813–20.
[89]. Shimizu H, Kumabe T, Shirane R, Yoshimoto T et al. Correlation between choline level measured by proton MR spectroscopy and Ki-67 labeling index in gliomas. Am J Neuroradiol. 2000;21:659–665 .
[90]. Nelson JS, Tsukada Y, Schoenfeld D, Fulling K, Lamarche J, Peress N. Necrosis as a prognostic criterion in malignant supratentorial, astrocytic gliomas. Cancer. 1983;52:550–554.